Structural Chemistry of Multi-Copper Oxidase

Ph.D. thesis

Mahfuza Akter

SD13L005

Abstract

Multicopper oxidases oxidize various phenolic and nonphenolic compounds by using molecular oxygen as an electron acceptor to produce water. A multicopper oxidase protein, CueO, from *Escherichia coli* is involved in copper homeostasis in the bacterial cells. Although X-ray crystallographic studies have been conducted, the reduction mechanism of oxygen and the proton transfer pathway remain unclear owing to the difficulty in identifying hydrogen atoms from X-ray diffraction data alone. To elucidate the reaction mechanism by neutron crystallography, a preparation system for obtaining large, high-quality single crystals of deuterated CueO was developed. Tiny crystals were obtained from the deuterated CueO initially prepared from the original construct. The X-ray crystal structure of the deuterated CueO showed that the protein contained an incompletely truncated signal sequence at the N-terminus, which resulted in the heterogeneity of the protein sample for crystallization. Here, a new CueO expression system that had a HRV3C cleavage site just after the signal sequence was constructed. Deuterated CueO from the new construct was expressed in the cells cultured in deuterated algae extract medium, and the signal sequence was completely eliminated by HRV3C protease. The deuteration level of the purified protein was estimated by MALDI-TOF mass spectrometry to be at least 83.2% compared with the non-deuterated protein. Non-deuterated CueO crystallized in the space group $P2_1$ with cell dimensions of a = 49.51 Å, b = 88.79 Å, c = 53.95 Å, and β = 94.24°, and deuterated CueO crystallized in the space group $P2_12_12_1$ with cell dimensions of a = 49.91 Å, b = 106.92 Å, and c = 262.89 Å. The crystallographic parameters from the new construct were different from previously reported non-deuterated crystals. The non-deuterated and deuterated CueO from the new construct had similar UV-Vis spectra, enzymatic activities, and overall

structure and geometry of the ligands to the copper atoms in the active site to those of previously reported CueOs. These results indicate that the CueO protein prepared by the new construct is suitable for further neutron diffraction studies.

Table of Contents

Contents **Page No.**

1. Introduction……..…..…. 6

1.1. Multicopper oxidases……..... 6

1.2. CueO……..... 8

1.3. Neutron crystallography……..... 10

1.4. Neutron crystallography of CueO……..... 12

1.5. Objectives of this study……..... 13

2. Materials and method……..... 14

2.1. Construction of expression plasmid……..……...…… 14

2.2. Effect of temperature on the expression of pASK-IBA3plus-wtCueO (original expression system) in deuterated medium…….…..... 16

2.3. Effect of detergents to extract oCueO-d from the pellet……...…… 16

2.4. Effect of AHT concentration on the expression of oCueO-d……....…… 16

2.5. Expression of pASK-IBA3plus-wtCueO (original construct) in deuterated medium and purification of oCueO-d……..…….……... 16

2.6. Expression of pASK-IBA3plus-HRV3C-wtCueO (new construct) in LB (Luria-Bertani) medium and purification of CueO-h…….……..... 17

2.7. Expression of pASK-IBA3plus-HRV3C-wtCueO (new construct) in

deuterated medium and purification of CueO-d……..…….….. 18
2.8. Final protein sample preparation…….……. 19
2.9. Absorption spectra…….. 20
2.10. Biochemical assay…….……. 20
2.11. Mass spectroscopy……. 21
2.12. Crystallization…… 21
2.12.1. Screening of the crystallization condition for oCueO-h and CueO-h…….. 21
2.12.2. Optimization of the precipitants for oCueO-h and CueO-h……..…….…. 22
2.12.3. Crystallization of the oCueO-d and CueO-d…….….. 23
2.13. X-ray diffraction experiment……..… 23
2.14. Refinement of protein structure models……..… 23
3. Results and Discussion……. 25
3.1. Construction of expression plasmid…….. 25
3.2. Effect of temperature on the expression of pASK-IBA3plus-wtCueO (old construct) in deuterated medium……..…….…… 25
3.3. Effect of detergents to extract oCueO-d from the pellet……...…… 26
3.4. Effect of AHT concentration to get soluble protein in supernatant…….. 27
3.5. Expression of pASK-IBA3plus-wtCueO (old construct) in deuterated medium and purification of oCueO-d……..…….…… 28
3.6. Expression of pASK-IBA3plus-HRV3C-wtCueO (new construct) in LB (Luria-Bertani) medium and purification of CueO-h……...……... 29
3.7. Expression of pASK-IBA3plus-HRV3C-wtCueO (new construct) in deuterated medium and purification of CueO-d…….……..… 32
3.8. Expression, purification and final protein sample preparation……. 33

3.9. Absorption spectra…… 35

3.10. Enzymatic activity…… 35

3.11. Deuteration level determined by mass spectrometry…… 36

3.12. Crystallization…… 39

3.12.1. Screening of the crystallization condition for oCueO-h and CueO-h…….. 39

3.12.2. Optimization of the precipitants for oCueO-h and CueO-h……..…….. 41

3.12.3. Crystals of the oCueO-d and CueO-d……...…… 42

3.13. X-ray diffraction experiment……...…… 43

3.14. X-ray structures of oCueO-d, CueO-h, and CueO-d…….....…….. 43

3.15. Comparison of the X-ray structures of oCueO-d, CueO-d, and CueO-h…..… 47

3.16. Structure of the copper centers…… 48

4. Conclusions…….. 51

5. References…… 52

6. Acknowledgements…… 61

1. Introduction

1.1. Multicopper oxidases

Multicopper oxidases (MCOs) which are involved in various functions of copper and iron metabolism to polyphenol oxidation, are a widely distributed class of enzymes. They are copper-containing proteins with a cupredoxin-like domains as a structural unit. According to the number of domains, they have been classified into three groups: the two-domain type (2dMCO), the three-domain type (3dMCO) and the six-domain type (6dMCO) (Komori & Higuchi, 2010). Among these three types of MCOs, 3dMCO is the main group of MCO which consists of three cupredoxin-like domains. There are various types of 3dMCOs, including laccases and several oxidases with specific substrates such as ascorbate, copper, iron or bilirubin. All of the 3dMCO enzymes share similar spectroscopic properties which are related to the copper ions in the active site. MCOs consist of four copper ions in the active site which is arranged in two parts: a blue type I mononuclear copper center (T1Cu) and a trinuclear copper center (TNC) containing the other three copper atoms: a type II copper (T2Cu) and a pair of type III coppers (T3Cu; T3aCu and T3bCu) (Solomon, *et al*., 1996; Grass & Rensing, 2001; Komori, *et al*., 2012). The types I, II and III of copper are characterized on the basis of optical and electromagnetic resonance (EPR) spectroscopic properties. T1Cu has an absorption peak around at 600 nm, and a narrow hyperfine coupling in EPR spectra. This copper atom is coordinated by three strong ligands (one cysteine and two histidines) and one weaker ligand (typically a methionine), and constitutes a distorted tetrahedral coordination system. An extremely intense absorption due to the charge transfer transition between the copper atom and the cysteine ligand is responsible for the deep blue color of this enzyme. On the other hand, T2Cu is generally

coordinated with two histidines and a water–oxygen and it possesses a much weaker absorption, broader hyperfine interactions. However, T3Cu is accompanied with an absorbance band at 330 nm and is usually coordinated by three histidines per copper and a bridging moiety. It is an EPR non-detectable copper pair (antiferromagnetically coupled) (Adman, 1991; Solomon, *et al*., 1996). TNC is the active site responsible for dioxygen reduction(Bento *et al*., 2005; Sakurai & Kataoka, 2007; Solomon *et al*., 2008). Through the sequence segment (His-Cys-His), the T1Cu site is connected with-TNC and the distance between them is approximately 12 Å.

MCOs oxidize various phenolic and nonphenolic compounds using molecular oxygen as an electron acceptor to produce water. All of the copper atoms of MCOs are engaged with the transfer of electrons from the substrate to O_2 which is the final electron acceptor **(Fig.1)**. Electron transfer between the substrate and TNC is mediated by T1Cu. Since MCOs have broad substrate specificity, they can be used in a variety of biotechnological applications, such as textile dye bleaching, pulp bleaching, polymer synthesis and bio-electrodes.

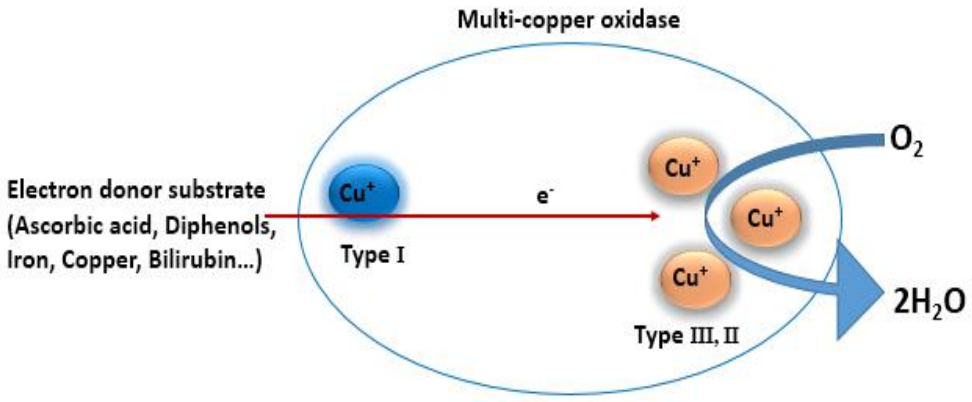

Fig.1. A schematic diagram of the catalytic mechanism of multi-copper oxidase

1.2. CueO

CueO (previously called yacK) (Grass & Rensing, 2001; Kim *et al.*, 2001; Ueki *et al.*, 2006) is one of 3dMCO, and is expressed to the periplasmic space in *Escherichia coli* (Djoko *et al*, 2010). It is involved in the copper homeostasis in *E. coli* with a molecular weight of 53.4 kDa (Outten *et al.,* 2001; Rensing & Grass, 2003; Roberts *et al.*, 2002). CueO is also important as the cathodic enzyme of bio-fuel cell in addition with the Cu efflux system of *E. coli* (Grass & Rensing, 2001; Komori *et al.*, 2012). It has a broad substrate specificity like most MCOs for organic molecules such as catechols, iron-chelating siderophores, 2,2'-azino-bis(3-ethylbenzothiazoline-6-sulfonic acid) (ABTS), *p*-phenylenediamine, and the chromophoric model substrate 2,6-dimethoxyphenol. Toward these substrates, the enzymatic activities of CueO are notably low but are considerably enhanced in the presence of excess Cu(II) ions (Grass & Rensing, 2001; Kim *et al.*, 2001). It is already known that CueO is capable to protect the periplasmic enzymes such as alkaline phosphatase from copper-induced toxic reactions (Grass & Rensing, 2001), indicating that one of the biological roles of CueO is the periplasmic detoxification of copper. However, the exact mechanism of this protection is still unknown. It has been proposed by several groups (Outten *et al*., 2001; Grass & Rensing, 2001) that the periplasmic more toxic Cu(I) is oxidized by the CueO to the less toxic Cu(II) and thereby directly protecting the organism from copper-induced damage. CueO not only possessed the oxidase activity but also exhibited the ferroxidase activity (Grass & Rensing, 2001). All of these properties make CueO an interesting model system to study bacterial multi-copper oxidases.

Several X-ray crystal structures of CueO were already determined by different groups [pdb code: 1KV7 (Roberts *et al.,* 2002), 1N68, 1PF3 (Roberts *et al.,*

2003), 2FQD, 2FQE, 2FQF, 2FQG (Li *et al.,* 2007), 2YXV, 2YXW (Kataoka *et al.,* 2007), 3UAA, 3UAB, 3UAC, 3UAD, 3UAE (Komori *et al.,* 2012)]. The crystal structures showed that CueO is composed of three repeated pseudoazurin domains with one T1Cu site in domain 3 and one TNC between domains 1 and 3 **(Fig.2)** (Roberts *et al.,* 2002).

Like other MCOs, the metal active site of CueO is also composed of four copper atoms,

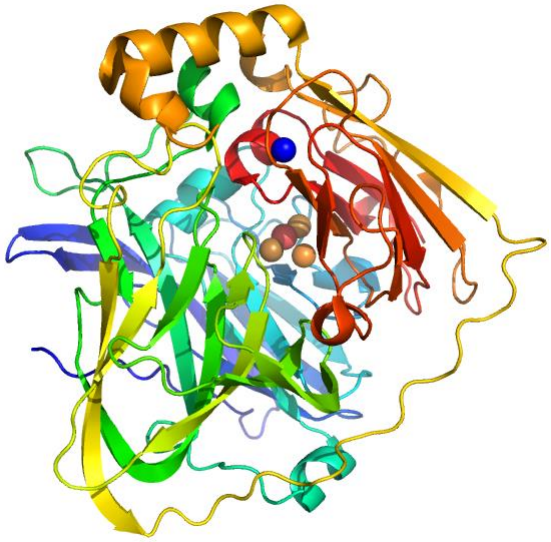

Fig.2. A ribbon representation of the published hydrated wild type CueO with the T1 Cu (blue),trinuclear copper center, TNC (orange), and TNC bridging oxygen atom (red) shown as space-filling spheres. The figure was decorated with PyMOL (DeLano, 2002) using the coordinates from Protein Data Bank file 1KV7.

T1Cu, T2Cu, and T3Cu. Although the X-ray crystal structure of CueO was already determined, the reaction mechanism is not yet understood well and it is very difficult to predict without knowing the protonation states of the active site residues. Another crystallography method, such as neutron crystallography, is required to know the protonation states of the active site residues.

1.3. Neutron crystallography

Neutron crystallography is a powerful technique which is used to locate hydrogen and can easily provide information on the protonation states of amino-acid residues and ligands, identification of solvent molecules and the nature of bonds involving hydrogen (Niimura & Bau, 2008). It is difficult to get a positional information of hydrogen atoms in the enzyme active site by X-ray structure analysis. On the other hand, neutron structure analysis can reveal the positional information of enzymatically critical protons and the detailed feature of hydrogen bonding networks, thus providing novel insights into the enzyme catalytic mechanism (Budayova-Spano *et al*., 2007).

In biological structures, neutron crystallography can locate the positions of hydrogen atoms at moderate resolutions of 1.5–2.2 Å (Schoenborn, 1969; Kossiakoff, *et al.*, 1980; Phillips & Schoenborn, 1981). This is because the neutron scattering length does not depend on the atomic number, but neutrons are scattered by atomic nuclei, rather than by electrons (Flora *et al.,* 2013). Moreover, the neutron scattering lengths of hydrogen and deuterium are similar to those of the 'heavier' atoms carbon, oxygen, and nitrogen, and both atoms are easily detected in the neutron scattering length density maps. Therefore, neutron structure analysis is very useful to determine the protonation states of catalytic residues in enzymes (Coates *et al*., 2008; Blakeley *et al.,* 2008; Adachi *et al.,* 2009; Glusker *et al.,* 2010; Tomanicek *et al.,* 2011; Fisher *et al.*, 2012; Kovalevsky *et al.,* 2012) and precise hydrogen-bonding and ligand-binding features in proteins. In addition, since neutron radiation used in the crystallographic experiments are uncharged and have thermal energies of just a few meV, neutron diffraction does not cause radiation-damage in protein crystals and structures are routinely determined at room temperature, that can be of concern in X-ray crystallography. The main drawback

of neutron crystallography is that it requires either big crystals or very long exposure times in order to have a measurable diffraction signal because of the relatively low flux of available neutron beams (Myles *et al*., 1998; Bon *et al*., 1999; Coates *et al*., 2001). But The required crystal volume, however, can be numerously reduced, if the protein is completely perdeuterated (all hydrogen atoms are replaced by deuterium atoms). The reason is deuteration can change the scattering contrast of specific parts of a macromolecule and also can enhance its scattering properties (Blakeley *et al*., 2008). In addition, the large incoherent scattering background of hydrogen is significantly reduced by per-deuteration which provides a large gain in the signal-to-noise ratio of diffraction images (Gamble *et al*., 1994; Shu *et al*., 2000; Hazemann *et al*., 2005). Moreover, deuterium atoms are more easily visualized than hydrogen atoms in the neutron scattering length density maps, because of the neutron scattering length of deuterium is positive and twice (+6.67) in magnitude than that of hydrogen (-3.74) (Shu *et al*., 2000). There are some ways to get the partially- or fully(per)-deuterated protein crystals for neutron diffraction study. Partially-deuterated crystals are obtained from non-deuterated protein samples. This can be done by preparing the non-deuterated crystals from the mother liquor prepared in D_2O or soaking the crystals grown in H_2O into a mother liquor prepared in D_2O. Fully- or per-deuterated crystals can be obtained by using the protein samples expressed in deuterated media in D_2O. For this purpose, new expression system should be developed by using an appropriate vector in a host cell which effectively expresses the recombinant protein and crystallization condition should be rescreened. Since partially-deuterated crystals provide poor signal-to-noise ratio of diffraction image, fully- or per-deuterated protein crystals are more favorable.

1.4. Neutron crystallography for CueO

MCOs are very prospective to use in biofuel cells as cathodic enzyme, due to this efficient dioxygen reduction system (Miura *et al*., 2007; Tsujimura *et al.*, 2008; Miura *et al.,* 2009). Two reaction intermediates are comprised in this reduction system and these intermediates are known as intermediate I (peroxide intermediate) and intermediate II (native intermediate) **(Fig.3)** (Bento *et al*., 2005; Sakurai & Kataoka, 2007; Komori *et al*., 2012). However, still the reaction mechanism of this reduction system is not fully understood because there is no clear evidence to support the presence of peroxide at TNC, though the X-ray crystal structures of CueO were already determined at high resolution.

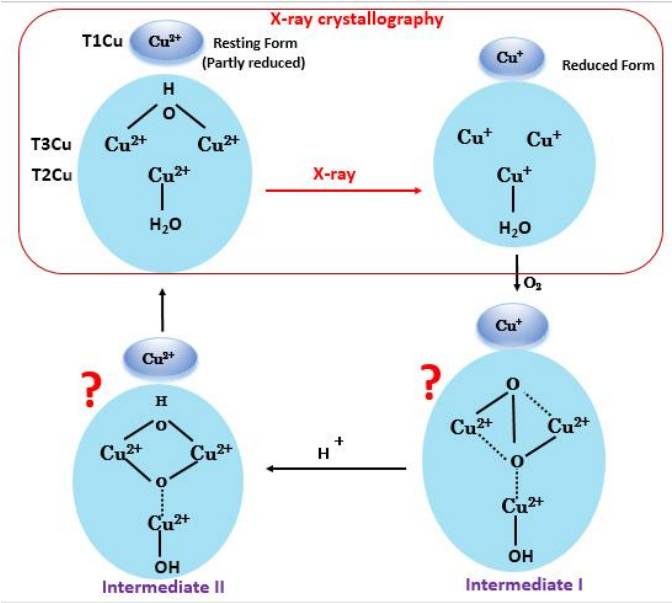

Fig.3. The proposed reaction process of multi-copper oxidase where the intermediates I and II are also familiar as the peroxide intermediate and native intermediate, respectively.

This is caused by the difficulty of the assignment of hydrogen atoms and protonation states of the residues which are responsible for the catalytic reaction, and unfavorable radiation damage and dose reduction of the active site by X-ray beam. In order to

clearly demonstrate the reaction mechanism of CueO, it is necessary to identify the protonation states of the active site residues and to clearly recognize the hydrogen-bonding network in the surrounding of the catalytic residues. By the neutron crystallographic experiment, it is possible to understand the enzyme-reaction mechanisms (Kossiakoff & Spencer 1981; Coates *et al*., 2008; Blakeley *et al.,* 2008; Adachi *et al.,* 2009; Glusker *et al.,* 2010; Tomanicek *et al.,* 2011; Fisher *et al.*, 2012; Kovalevsky *et al.,* 2012).

1.5. Objectives of this study

For neutron diffraction, fully- or per-deuterated crystal is favorable to avoid an incoherent signal, which significantly reduces signal-to-noise ratios, from hydrogen atoms of the protein. During the preparation of the deuterated CueO obtained from the original expression system, I found an incompletely truncated signal sequence at the N-terminus of CueO. This additional heterogeneous sequence may hamper the well-ordered crystal packing of the molecules that is necessary for obtaining large single crystals suitable for neutron diffraction.

In this work, I designed a new construct by adding a human Rhinovirus 3C (HRV3C) protease cleavage site after the signal sequence, and prepared deuterated CueO (CueO-d) without the signal sequence and its crystals in D_2O. I also obtained the enzymatic activity, UV-Vis spectra, and X-ray crystal structures of non-deuterated CueO (CueO-h) and CueO-d from the new construct, and deuterated CueO from the original construct (oCueO-d) to confirm that there were no major differences in the active site and overall structures caused by the deuteration of the protein.

2. Materials and method

2.1. Construction of expression plasmid

The expression plasmid for C-terminal Strep-Tagged wild type CueO (Kataoka *et al.*, 2007) (pASK-IBA3plus-wtCueO) was constructed using pASK-IBA3plus (IBA GmbH) linearized with BsaI restriction endonuclease. The expression plasmid for HRV3C-CueO carrying a modified Twin-Strep-tag followed by a HRV3C protease recognition site, inserted between residues Ala28 and Ala29, was constructed from the expression plasmid for wild-type CueO from *E. coli* **(Table 1)**. A nucleotide fragment coding for the mature region of CueO was amplified by PCR using primers HRV3C-GG-CueO_A29-F (5′-CTGTTCCAGGGGCCCGGCGGTGCAGAACGCCCAACGTTACC-3′) and CueO-stopstop_pASKIBA3-R (5′-CACAGGTCAAGCTTATTATACCGTAAACCCTAACATCATCC-3′), where underlined characters indicate overlap sequences assembled by In-Fusion (Clontech Laboratories) and Q5 Hot Start DNA polymerase (New England Biolabs Inc.). A fragment encoding the modified Twin-Strep-tag and HRV3C recognition sequences was obtained by PCR using primers STrEP-f (5′-TGGAGCCACCCGCAGTTC) and HRV3C-r (5′-GGGCCCCTGGAACAGAACTTC-3′) from a modified pColdI vector (Takara Bio, Inc.) containing 6xHis, Twin-Strep-tag, and the HRV3C recognition site (Data not shown). The signal peptide region (Met1-Ala28) of CueO and the vector parts were amplified by inverse PCR using primers stopstop_pASKIBA3-F (5′-TAATAAGCTTGACCTGTGAAGTG-3′) and CueO_E30_STrEP-R (5′-CTGCGGGTGGCTCCAACTACCGCCACTTGCCGCAAATACTGCGCG-3′) from pASK-IBA3plus-CueO. The resulting PCR products were assembled by using In-Fusion

to generate a circular plasmid. Each plasmid was transformed into *E. coli* BL21 (DE3) cells.

Table 1. DNA and amino acid sequence of HRV3C-CueO.

	Sequence
DNA of tag part	GCAAGTGGCGGTAGT**TGGAGCCACCCGCAGTTCGAGA** **AA**GGTGGAGGTTCCGGAGGTGGATCGGGAGGTGGATCG **TGGTCTCATCCGCAATTTGAGAAGG**GGTTCAACTAGTGG TCTGGAAGTTCTGTTCCAGGGGCCCGGCGGT
Whole protein	MQRRDFLKYSVALGVASALPLWSRAVFAASGGS**WSHPQF** **EK**GGGSGGGSGGGS**WSHPQFEK**GSTSGLEVLFQGPGGAE RPTLPIPDLLTTDARNRIQLTIGAGQSTFGGKTATTWGYNG NLLGPAVKLQRGKAVTVDIYNQLTEETTLHWHGLEVPGEV DGGPQGIIPPGGKRSVTLNVDQPAATCWFHPHQHGKTGRQ VAMGLAGLVVIEDDEILKLMLPKQWGIDDVPVIVQDKKFS ADGQIDYQLDVMTAAVGWFGDTLLTNGAIYPQHAAPRGW LRLRLLNGCNARSLNFATSDNRPLYVIASDGGLLPEPVKVS ELPVLMGERFEVLVEVNDNKPFDLVTLPVSQMGMAIAPFD KPHPVMRIQPIAISASGALPDTLSSLPALPSLEGLTVRKLQLS MDPMLDMMGMQMLMEKYGDQAMAGMDHSQMMGHMG HGNMNHMNHGGKFDFHHANKINGQAFDMNKPMFAAAK GQYERWVISGVGDMMLHPFHIHGTQFRILSENGKPPAAHR AGWKDTVKVEGNVSEVLVKFNHDAPKEHAYMAHCHLLE HEDTGMMLGFTV

[a]Bold characters, single underlined and double underlined indicate Twin-Strep-tag, linker, and HRV3C protease recognition site, respectively.

2.2. Effect of temperature on the expression of pASK-IBA3plus-wtCueO (original construct) in deuterated medium

After transformations of expression construct into *E. coli* BL21 (DE3) strain, bacterial cells were cultured at 37 °C. When OD_{600} reached a value of 0.5, the culture was induced by 0.2 µg/ml anhydrotetracycline (AHT) at the temperature of 25 °C, 32 °C, and 37 °C to check the effect of temperature on the expression of wild type CueO protein (oCueO) in deuterated medium. After induction, the cultures of these three temperatures were separately incubated for 18 hours with shaking at 180 rpm.

2.3. Effect of detergents to extract oCueO-d from the pellet

After collection of supernatant, it was found that most of oCueO-d was not found in the supernatant, but localized at the pellet. In order to extract the protein from the pellet, three different detergents at 0.1 % concentration in the sonication buffer were used during purification. These three detergents were Triton X-100 (Sigma-Aldrich), Tween 80 (Sigma-Aldrich), and Brij35 (Sigma-Aldrich).

2.4. Effect of AHT concentration on the expression of oCueO-d

To check the effect of AHT concentration on the expression of oCueO-d protein, inoculation was carried out at three concentrations, 0.2, 0.1, and 0.05 µg/ml of AHT for 18 hours at 37 °C with shaking at 180 rpm in the fully deuterated medium.

2.5. Expression of pASK-IBA3plus-wtCueO (original construct) in deuterated medium and purification of oCueO-d

Expression construct of pASK-IBA3plus-wtCueO was transformed into *E. coli*

BL21 (DE3) strain. Cultivation was carried out in a deuterated algae extract (CELTONE-d, Spectra Stable Isotopes) expression system supplemented with 0.1 mg/mL sodium ampicillin at 37 °C. Protein expression was induced by the addition of 0.05 μg/mL AHT and 1 mM $CuSO_4$ when the OD600 reached a value of 0.5. After induction, the culture was incubated for 18 hours at 37 °C with shaking at 180 rpm.

After cell harvesting, the periplasmic fractions of the cells were prepared by cold osmotic shock using 20% (w/v) sucrose and 10 mM Tris-HCl pH 8.0. After centrifugation, protease inhibitor cocktail (Roche) containing 10 mM Tris-HCl pH 8.0 buffer was added to the periplasmic fractions to increase the yield of deuterated soluble protein. The supernatant containing the soluble protein was used for affinity chromatography by using a Strep-Tactin Sepharose affinity resin (IBA GmbH) column equilibrated with 50 mM Tris-HCl buffer pH 8.0. The same buffer was used to wash the column and fully-deuterated CueO was eluted with the same buffer supplemented with 2.5 mM desthiobiotin. After affinity chromatography, finally deuterated protein was further purified by size-exclusion chromatography using 20 mM Na-phosphate pH 6.0 buffer in HiLoad 16/60 Superdex 200 column (GE Healthcare). After the final purification step, the protein purity was judged by SDS-PAGE. All the protein bands in SDS-PAGE were stained by CBB in this study

2.6. Expression of pASK-IBA3plus-HRV3C-wtCueO (new construct) in LB (Luria-Bertani) medium and purification of CueO-h

After the transformation of pASK-IBA3plus-HRV3C-wtCueO into *E. coli* BL21 (DE3) strain, the cells were grown in LB (Luria-Bertani) medium supplemented with 0.1 mg/mL sodium ampicillin at 25 °C. When the OD600 reached a value of 0.5,

0.05 µg/mL AHT and 1 mM $CuSO_4$ were added to the culture to induce the expression of protein at 25 °C, then the culture of cells was incubated for 18 hours at 25 °C with shaking at 180 rpm.

After cell harvesting, the periplasmic fractions of the cells were prepared by cold osmotic shock using 20% (w/v) sucrose and 10 mM Tris-HCl pH 8.0. After centrifugation, protease inhibitor cocktail (Roche) containing 10 mM Tris-HCl pH 8.0 buffer was used to suspend the cells. Here, only cold osmotic shock was used to extract the non-deuterated soluble protein. The supernatant containing the soluble protein was used for affinity chromatography using a Strep-Tactin Sepharose affinity resin (IBA GmbH) column equilibrated with 50 mM Tris-HCl buffer pH 8.0. The same buffer was used to wash the column and non-deuterated CueO was eluted with the same buffer supplemented with 2.5 mM desthiobiotin. After affinity chromatography, the HRV3C protease sequence containing CueO protein was cleaved by overnight reaction with HRV3C enzyme at 1:20 ratio. After the reaction, the truncated signal sequence in the N-terminal part was removed by Strep-Tactin Sepharose affinity resin. Thereafter, non-deuterated protein was purified by ion exchange chromatography using a 5 ml HiTrap Q HP column (Bio Sciences) equilibrated with 10 mM Tris–HCl (pH 8.5) buffer. Target protein was eluted from the column with a linear gradient of NaCl (0–1.0 M) in the same buffer, then finally purified by size-exclusion chromatography as like as pASK-IBA3plus-wtCueO deuterated protein.

2.7. Expression of pASK-IBA3plus-HRV3C-wtCueO (new construct) in deuterated medium and purification of CueO-d

Expression of wild type CueO with HRV3C cleavage site (i.e.

pASK-IBA3plus-HRV3C-wtCueO) was carried out by using the same protocol as the old construct (i.e. pASK-IBA3plus-wtCueO) in deuterated medium. The protocol for the purification steps was slightly modified from that described in the section 2.5. After cell collection, suspension, sonication, and centrifugation, the supernatant was collected and purified by Strep-Tactin Sepharose affinity resin ((IBA GmbH). The eluted sample of affinity chromatography was then used for overnight reaction with HRV3C enzyme at 1:20 ratio to truncate the signal sequence in N-terminal part. After removing the truncated part from the main protein by Strep-Tactin Sepharose affinity chromatography then finally the target protein was purified by size-exclusion chromatography as like as oCueO-d protein.

2.8. Final protein sample preparation

In case of the final preparation of the non-deuterated protein (CueO-h), three steps of chromatography (affinity, ion-exchange, and size-exclusion) were required. The final purified sample in the 20 mM Na-phosphate pH 6.0 buffer was directly concentrated by using a Vivaspin 30 kDa MWCO (GE Healthcare). On the other hand, after the two steps of chromatography (affinity and size-exclusion), the fully-deuterated proteins (CueO-d and oCueO-d) were prepared by the buffer exchange from non-deuterated (20 mM Na-phosphate pH 6.0) to deuterated (20 mM Na- phosphate pD 6.0) buffer solutions. Concentration and dilution of deuterated CueO were repeated three times by centrifugation using a Vivaspin 6, 30 kDa MWCO (GE Healthcare).

2.9. Absorption spectra

UV-Vis absorbance spectra were recorded at room temperature at 250–800 nm by using a spectrophotometer (V-660, JASCO International Co., Ltd.). The measurements were performed using a cell with a 1 cm path length and a protein concentration of 1 mg/mL.

2.10. Biochemical assay

The enzymatic activities of CueO-d, CueO-h, and oCueO-d were assayed from the absorption increases at 420 nm (ε = 36,000 M^{-1} cm^{-1}) catalyzed by CueO at 25 °C, which corresponds to the absorption band for the typical oxidized product of 2,2′-azino -bis(3-ethylbenzothiazoline-6-sulfonic acid) (ABTS). Each reaction solution (1 mL) contained 6 mM ABTS, 1 mM $CuSO_4$, and 50 mM sodium acetate pH/pD 5.5 (or 5.1) buffer.

2.11. Mass spectroscopy

MALDI-TOF mass analysis was performed on an ultrafleXtreme mass spectrometer (Bruker Daltonics). Purified samples (0.5 mg/mL) were mixed with Super 2,5-dihydroxybenzoic acid (DHB) (2,5-DHB/2-hydroxy-5-methoxybenzoic acid 90:10, Sigma-Aldrich), deposited on a ground steel plate, and allowed to dry at room temperature. Mass calibration was performed by using bovine serum albumin (66.4 kDa) and Protein A (44.6 kDa). Mass spectra were obtained by the accumulation of 10,000 shots for each analysis and were processed by FlexAnalysis software (Bruker Daltonics).

2.12. Crystallization

2.12.1. Screening of the crystallization condition for oCueO-h and CueO-h

At the beginning stage of crystallization, commercial screening kits **(Table 2)** were used by sitting drop vapor diffusion method for screening of non-deuterated CueO proteins (oCueO-h and CueO-h) at three different temperatures (4, 10, and 20 ºC). The protein concentration of these two CueO samples was ca. 6 mg/mL in 20 mM Na-phosphate pH 6.0. Screening of the crystallization was performed to use protein-to-precipitant ratio of 1:1, 1 μL each in 96-well sitting drop plates (Greiner Bio-One).

Table 2. Screening kits used for the preliminary crystallization of oCueO-h and CueO-h.

Screening kits	1. PACT *premier* Eco Screen (Molecular Dimensions Limited, UK) 2. The PGA Eco Screen (Molecular Dimensions Limited, UK) 3. ProPlex Eco Screen (Molecular Dimensions Limited, UK) 4. The Stura Footprint Combination (Molecular Dimensions Limited, UK) 5. Wizard Precipitant Synergy (Rigaku Reagents, Inc.) 6. Wizard Classic (Rigaku Reagents, Inc.) 7. SaltRx HT (Hampton Research, USA) 8. JBScreen Classic HTS II (Jena Biosciences, Germany)
Protein concentration	6 mg/ mL
Protein: Precipitant	1 μL: 1 μL
Temperature	4 ºC, 10 ºC & 20 ºC

2.12.2. Optimization of the precipitants for oCueO-h and CueO-h

By initial screening, good crystals appeared in the several kits. Among them, the kits which produced a few precipitates in the mother liquor **(Table 3)** were selected to perform further optimization in order to get best crystals in size and shape. During optimization, pH and PEG concentrations of the selected precipitants were optimized. In this crystallization step, the protein-to-precipitant ratio was 1:1 (5 µL each) and 24-well sitting drop Cryschem plates (Hampton Research) were used. By sitting drop vapor diffusion method, both oCueO-h and CueO-h (ca. 6 mg/mL) were used to optimize the conditions at two temperatures (4 and 20 ºC).

Table 3. Selected precipitant formulations of screening kits for optimization.

Precipitants	9A, 9C, 10C, 11A, 11B, 11C from PACT *premier*
	1F, 4C, 5C, 10E, 12E from ProPlex
	2D, 5G, 7A from the Stura Footprint Combination
	9D, 11C from Wizard Classic IV

2.12.3. Crystallization of the oCueO-d and CueO-d

Some of the best crystallization conditions for oCueO-h and CueO-h were used to crystallize the deuterated CueO proteins (oCueO-d and CueO-d). Besides sitting drop vapor diffusion method, micro-seeding was also performed to crystallize oCueO-d and CueO-d in some best selected crystallization conditions with a protein-to-precipitant ratio of 1:1, 5 µL in 24-well sitting drop Cryschem plates (Hampton Research). Both of the mother liquor (20 mM Na-phosphate pD 6.0) and outer solution were prepared in

D_2O. The crystallization was carried out with a final concentration of 6 mg/mL of CueO at 4 and 20 ºC.

2.13. X-ray diffraction experiment

The X-ray diffraction data sets for oCueO-d and CueO-h, CueO-d were collected at the BL38B1 beamline, SPring-8, Japan, by using a CCD detector (Q315, ADSC), and the NE3A beamline, Photon Factory, Japan, using a CCD detector (PILATUS 2M-F, Dectris). The crystals were cryoprotected by flash-soaking in the mother liquor supplemented with 15% (w/v) CryoProtX #3 solution containing 12.5% di-ethylene glycol, 12.5% ethylene glycol, 12.5% MPD, 12.5% 1,2-propanediol, 12.5% dimethyl sulfoxide, 12.5% glycerol, and 12.5mM NDSB201 (Molecular Dimensions Limited) for oCueO-d and 15% glycerol for CueO-h and CueO-d immediately before cooling to 100 K in a nitrogen gas stream on the beamline. Diffraction data sets were indexed, integrated, and scaled with the program HKL2000 (Otwinowski *et al*., 1997).

2.14. Refinement of protein structure models

The structures were solved with the molecular replacement method by using the reported structure of CueO (PDB code; IKV7) (Roberts *et al*., 2002) as a template. The individual atomic coordinates were refined by PHENIX (Adams *et al*. 2010) and the model building was performed with Coot (Emsley *et al*. 2004). In the structures, water molecules were added automatically in Coot before being checked manually and refined. The atomic coordinates and structure factors were deposited in the Protein Data Bank,

with accession codes 5B7E for the oCueO-d, 5B7M for CueO-d, and 5B7F for CueO-h structure. The figures were prepared with PyMOL (DeLano, 2002).

3. Results and Discussion

3.1. Construction of Expression Plasmid

The old construct of wild type CueO (Kataoka *et al*, 2007) contains the one Strep-Tag in the C-terminal site. On the other hand, the new construct of wild type CueO (HRV3C-wtCueO) was successfully made by insertion of a modified Twin-Strep-tag and a HRV3C protease recognition site in the N-terminal location **(Fig.4)**. The Twin strep-tag increases the affinity of the HRV3C-wtCueO protein to Strep-Tactin Sepharose resin, which is effective to separate the cleavage part from the main protein part during purification.

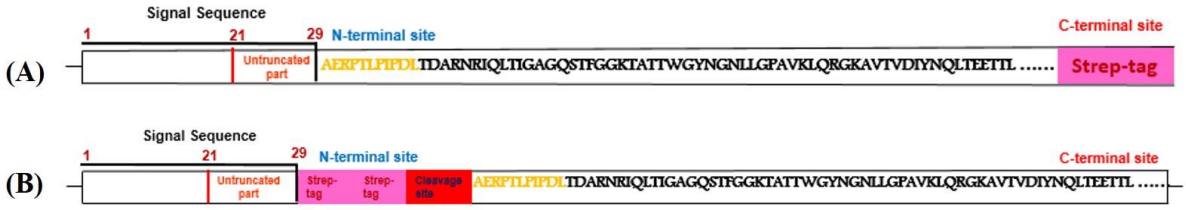

Fig.4. Structures of (A) old construct, pASK-IBA3plus-wtCueO (oCueO) and (B) new construct, pASK-IBA3plus-HRV3C-wtCueO (CueO). The expression vector for both of the constructs is pASK-IBA3plus (iba-lifesciences).

3.2. Effect of temperature on the expression of pASK-IBA3plus-wtCueO (old construct) in deuterated medium

After the inoculation of cell collection, suspension, sonication and centrifugation, the supernatant and pellet were separated and collected. It was confirmed that there was no significant difference on the expression of pASK-IBA3plus-wtCueO in deuterated medium at three different temperatures (25 °C, 32 °C, and 37 °C) by SDS-PAGE **(Fig.5)**. However, protein expression was little bit higher at 37 °C than

other two temperatures, and supernatant contained low amount of protein and most of the protein went to the pellet **(Fig.5)**.

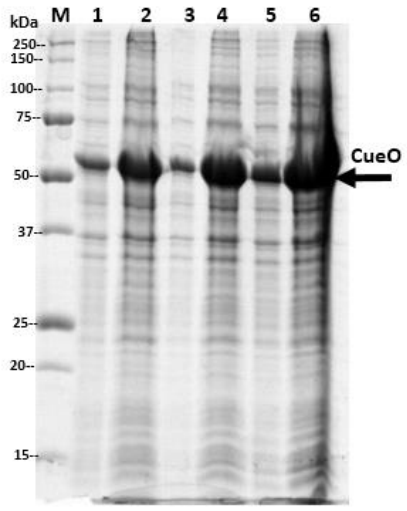

Fig.5. SDS-PAGE of expressed oCueO-d obtained from pASK-IBA3plus-wtCueO in deuterated medium (temperature effect on the expression). 1: Supernatant (25 °C), 2: Pellet (25 °C), 3: Supernatant (32 °C), 4: Pellet (32 °C), 5: Supernatant (37 °C), 6: Pellet (37 °C). "M" shows the "Standard protein marker (in kDa)".

3.3. Effect of detergents to extract oCueO-d from the pellet

Three detergents, Triton X-100, Tween 80, and Brij35 in the sonication buffer were used to extract oCueO-d in the fraction of the supernatant. As a result, there was no clear difference on the solubilization of protein **(Fig.6)**.

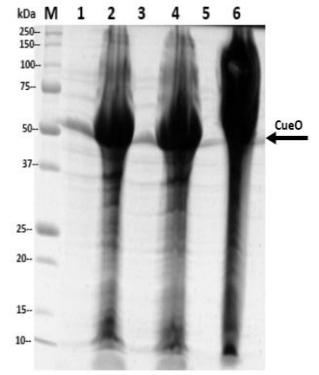

Fig.6. SDS-PAGE of solubilized CueO (effect of detergents). 1: Supernatant sample of Triton X-100, 2: Pellet sample of Triton X-100, 3: Supernatant sample of Tween 80, 4: Pellet sample of Tween 80, 5: Supernatant sample of Brij35, 6: Pellet sample of Brij35. "M" shows the "Standard protein marker (in kDa)".

3.4. Effect of AHT concentration on the expression of oCueO-d

After separation of the supernatant and pellet of oCueO-d induced by three different AHT concentrations (0.05 µg/mL, 0.1 µg/mL, and 0.2 µg/mL) in deuterated medium, it seemed that if protein was expressed by 0.05 µg/mL and 0.1 µg/mL AHT than it was possible to get solubilize protein in the supernatant **(Fig.7 A)**. However, it was not possible to get enough amount of protein in the supernatant when protein was expressed by 0.2 µg/mL AHT **(Fig.7 B)**. This suggests that protein expression was too high and Cu could not bind properly during protein folding, and also most of the holo-protein went to the pellet at 0.2 µg/mL AHT.

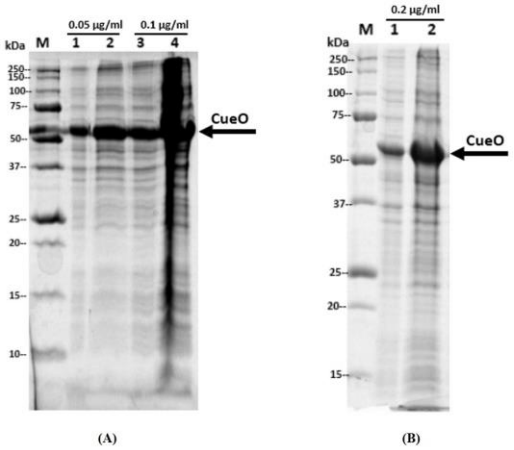

Fig.7. SDS-PAGE of expressed CueO (effect of AHT concentration). 1: Supernatant sample, 2: Pellet sample. "M" shows the "Standard protein marker (in kDa)".

3.5. Expression and purification of pASK-IBA3plus-wtCueO (old construct) in deuterated medium for crystallization

pASK-IBA3plus-wtCueO protein was expressed in deuterated medium and directly purified by two steps chromatography; Strep-Tactin affinity **(Fig.8)** and size-exclusion chromatography **(Fig.9 A and B)** without any enzymatic cleavage reaction.

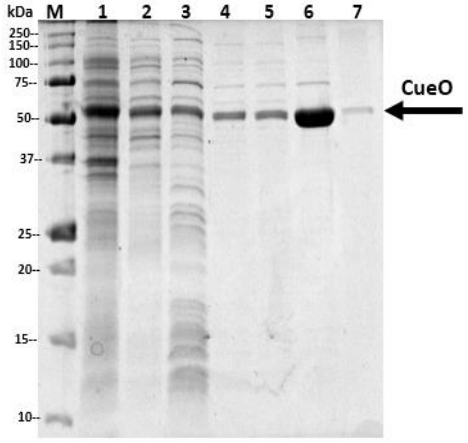

Fig.8. SDS-PAGE of purified oCueO-d by affinity chromatography (Strep-Tactin Sepharose resin). 1: Supernatant sample, 2: Flow through sample, 3: Washing sample, 4: Eluted sample 1, 5: Eluted sample 2, 6: Eluted sample 3, 7: Eluted sample 4. "M" shows the "Standard protein marker (in kDa)".

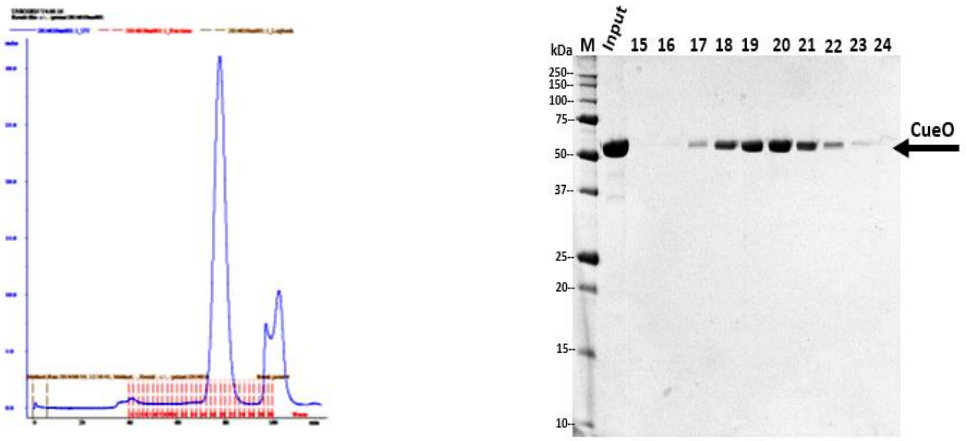

(A) (B)

Fig.9. Elution pattern of the size-exclusion chromatography (A) of oCueO-d (HiLoad 16/60 Superdex 200 column) and SDS-PAGE (B) of the fractions. Numbers indicate the different fractions volume of final purified eluted samples. "M" shows the "Standard protein marker (in kDa)".

3.6. Expression and purification of pASK-IBA3plus-HRV3C-wtCueO (new construct) in LB (Luria-Bertani) medium

To get non-deuterated CueO (CueO-h), the HRV3C cleavage site containing wild type CueO was expressed in LB medium. **Fig.10** shows results of SDS-PAGE of CueO-h after 1st step of purification by affinity chromatography. The obtained protein fractions were cleaved by overnight reaction with HRV3C enzyme, and purified by affinity chromatography again (**Fig.11**).

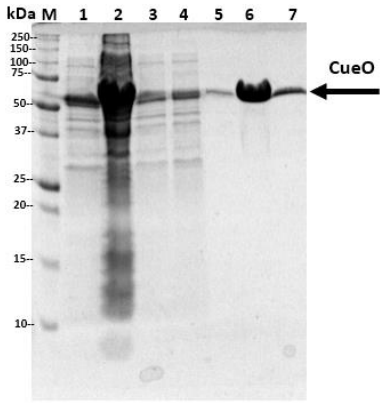

Fig.10. SDS-PAGE of the purified CueO-h by affinity chromatography (Strep-Tactin Sepharose resin). 1: Supernatant sample, 2: Pellet sample, 3: Flow through sample, 4: Washing sample, 5: Eluted sample 1, 6: Eluted sample 2, 7: Eluted sample 3. "M" shows the "Standard protein marker (in kDa)".

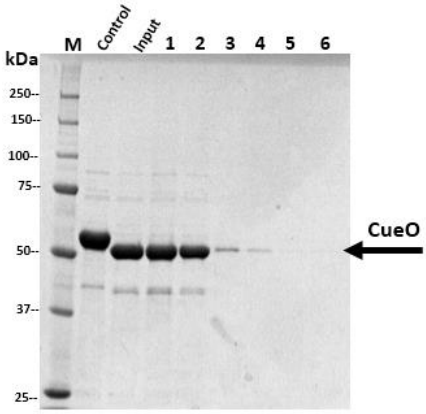

Fig.11. SDS-PAGE of enzymatically digested and purified CueO-h by affinity chromatography (Strep-Tactin Sepharose resin). CueO protein containing HRV3C cleavage site, Input: CueO protein after cleavage by HRV3C protease, 1: Flow through sample of cleavage reaction, 2: Washing sample 1 of cleavage reaction, 3: Washing sample 2 of cleavage reaction, 4: Washing sample 3 of cleavage reaction, 5: Eluted sample 1 of cleavage reaction, 6: Eluted sample 2 of cleavage reaction. "M" shows the "Standard protein marker (in kDa)".

After the second affinity chromatography, CueO-h was purified by

ion-exchange (**Fig.12**) and size-exclusion chromatography (**Fig.13**), respectively.

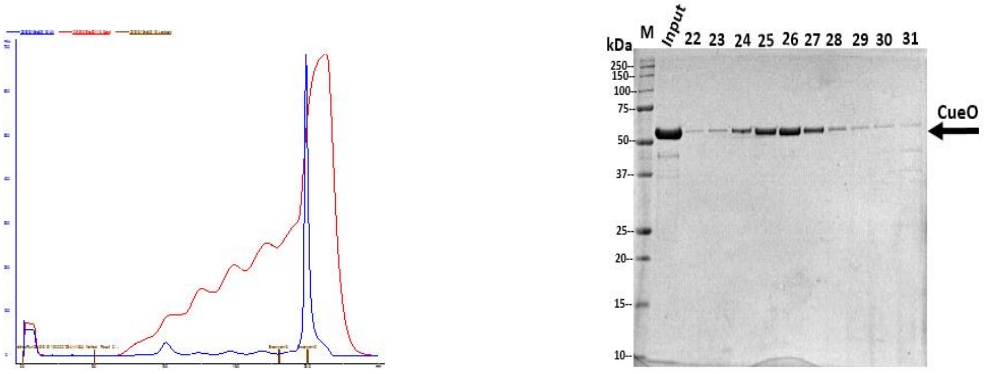

(A) (B)

Fig.12. Elution pattern of the ion-exchange chromatography (A) of CueO-h (5 ml HiTrap Q HP column) and SDS-PAGE (B) of the fractions. Numbers indicate the fraction numbers of the eluted samples. "M" shows the "Standard protein marker (in kDa)".

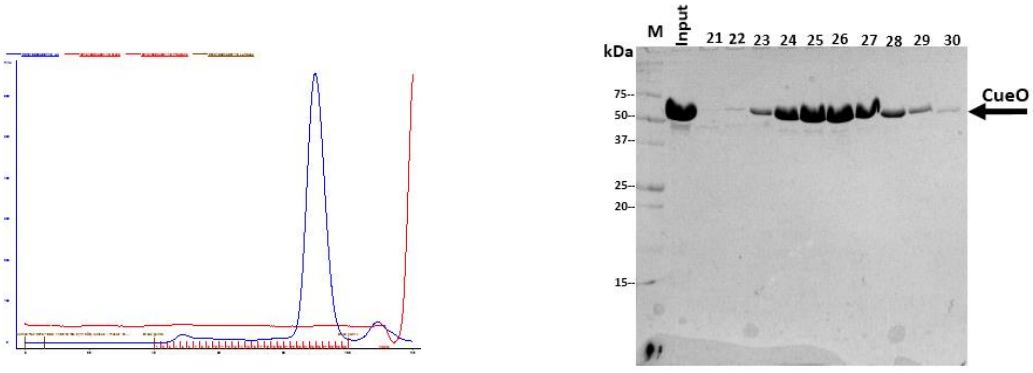

(A) (B)

Fig.13. Elution pattern of the size-exclusion chromatography (HiLoad 16/60 Superdex 200 column) CueO-h (A) and SDS-PAGE (B) of the fractions. Numbers indicate the fraction numbers of the eluted samples. "M" shows the "Standard protein marker (in kDa)".

3.7. Expression and purification of pASK-IBA3plus-HRV3C-wtCueO (new construct) in deuterated medium

The HRV3C cleavage site containing wild type CueO was expressed in deuterated algae extract (CELTONE-d, Spectra Stable Isotopes) medium, to prepare the deuterated protein. The results of affinity chromatography of CueO-d were shown in **Fig .14** and **Fig. 15** (after digestion).

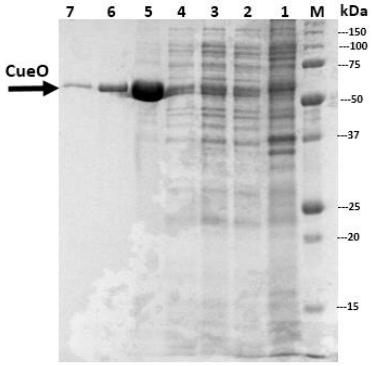

Fig.14. SDS-PAGE of the purified CueO-d by affinity chromatography (Strep-Tactin Sepharose resin). 1: Supernatant sample, 2: Flow through sample, 3: Washing sample, 4: Eluted sample 1, 5: Eluted sample 2, 6: Eluted sample 3, 7: Eluted sample 4. "M" shows the "Standard protein marker (in kDa)"

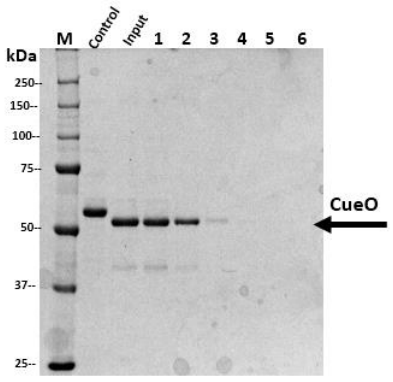

Fig.15. SDS-PAGE of enzymatically digested and purified CueO-d by affinity

chromatography (Strep-Tactin Sepharose resin). Control: CueO protein containing HRV3C cleavage site, Input: CueO protein after cleavage by HRV3C protease, 1: Flow through sample of cleavage reaction, 2: Washing sample 1 of cleavage reaction, 3: Washing sample 2 of cleavage reaction, 4: Washing sample 3 of cleavage reaction, 5: Eluted sample 1 of cleavage reaction, 6: Eluted sample 2 of cleavage reaction. "M" shows the "Standard protein marker (in kDa)".

Digested CueO-d was finally purified by size-exclusion chromatography **(Fig.16)**.

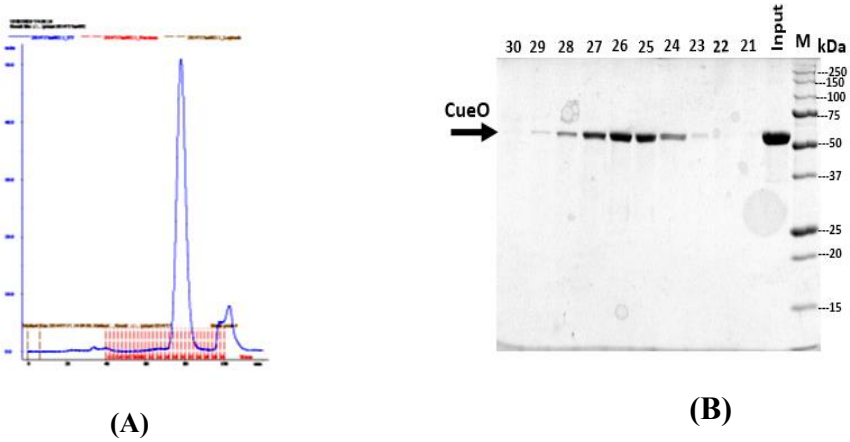

Fig.16. Elution pattern of CueO-d (A) by size-exclusion chromatography (HiLoad 16/60 Superdex 200 column) and SDS-PAGE (B) of the CueO-d fractions. Numbers indicate the fraction numbers of the eluted samples. "M" shows the "Standard protein marker (in kDa)".

3.8. Expression, purification and final protein sample preparation

The expression temperature of HRV3C-CueO-h was 25 °C; however, HRV3C-CueO-d was not expressed well at this temperature in CELTONE-d medium at this temperature. Good expression was observed when the cells were grown at 37 °C. Although the expression temperature was different, the total yields per liter from the two types of medium were similar (ca. 1.5 mg/L for CueO-h and 1.3 mg/L for CueO-d).

To maximize the recovery of the protein from the cells, osmotic shock and sonication were used for CueO-d, whereas only osmotic shock was sufficient for CueO-h. Affinity, ion-exchange, and size-exclusion chromatography were required to obtain sufficiently purified CueO-h for crystallization. However, for CueO-d, two chromatography steps were enough to obtain a crystallization-grade protein sample **(Fig. 17).**

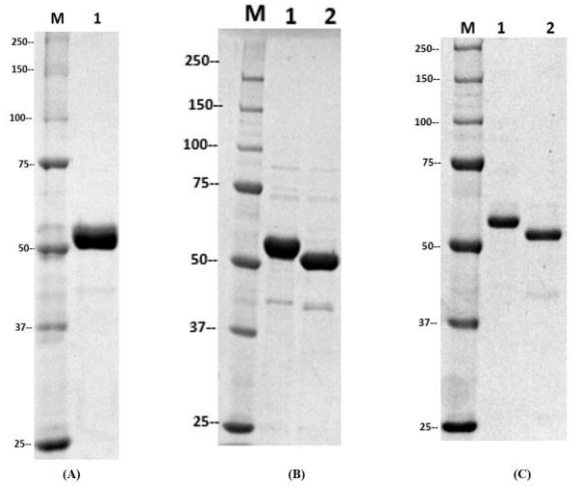

Fig.17. SDS–PAGE analysis of final purified oCueO-d, CueO-h, and CueO-d. A) 10% SDS-PAGE for wild-type oCueO-d (original construct). Lane M, protein markers (kDa). Lane 1, purified oCueO-d protein with partially truncated signal sequence at the N-terminal site. **B)** 10% SDS-PAGE for CueO-h. Lane M, protein markers (kDa). Lane 1, HRV3C-CueO protein. Lane 2, final purified CueO-h protein. **C)** 10% SDS-PAGE for CueO-d. Lane M, protein markers (kDa). Lane 1, HRV3C-CueO protein. Lane 2, final purified CueO-d protein.

3.9. Absorption spectra

The UV-Vis spectra of oCueO-h, oCueO-d, CueO-h, and CueO-d were similar **(Fig. 18)**, indicating that the introduction of the HRV3C cleavage site did not alter the structure of the T1Cu site of the enzyme. However, the peak height ratios between 330 nm (which is derived from type III copper) and other peaks vary each preparation of the enzyme. Though the reason for the peak height variation around 330 nm is unknown but it believes that the present samples are intact since they all have similar specific activities to the reported one.

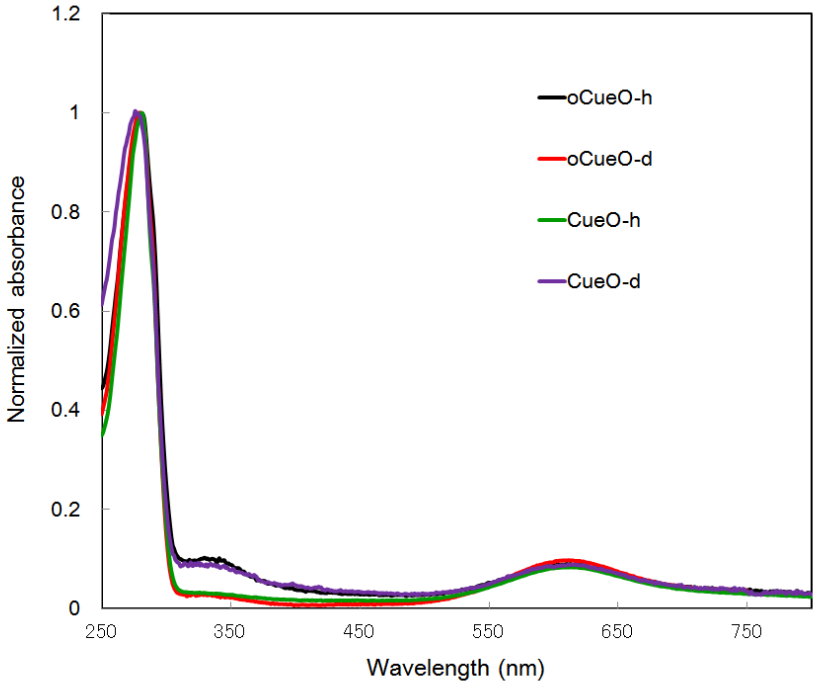

Fig. 18. UV-Vis spectra of oCueO-h, oCueO-d, CueO-h, and CueO-d.

3.10. Enzymatic activity

Comparing the enzymatic activity of oCueO-h, CueO-h, and CueO-d, CueO-d showed lower value in less than 10% than the others **(Fig. 19)**. This is probably due to the deuteration of protein, but the negative influence of deuteration on the activity small, suggesting that CueO-d prepared the present method is as intact as oCueO-h and CueO-h.

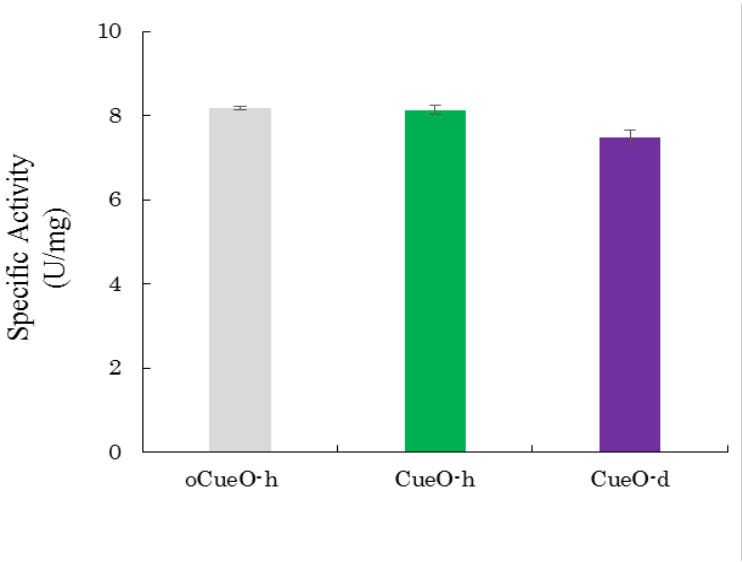

Fig. 19. Enzymatic activity of oCueO-h, CueO-h, and CueO-d.

The activities are shown as mean values with standard deviations calculated from triplicate experiments. Specific activities are expressed as units of activity per milligram of protein, where one activity unit represents 1 μmol of ABTS oxidized per min. Error bars indicate mean standard deviation of three independent measurements.

3.11. Deuteration level determined by mass spectrometry

The mass spectra for CueO-d and CueO-h are shown in **Figs. 20 A** and **20 B**, respectively. The molecular mass and the total number of the hydrogen atoms of HRV3C cleaved CueO-h were predicted to be 53,654 and 3729, respectively, by Protein

Calculator v3.4 (http://protcalc.sourceforge.net/) **(Table 4)**. The average mass value (53,752.7 Da) of three separate measurements for CueO-h was in good agreement with the predicted mass. The deuteration ratio of CueO-d can be estimated by the difference in masses between CueO-d and CueO-h. However, it is difficult to estimate the accurate ratio since CueO-d was purified in the H_2O-based buffer with which the exchangeable deuterium atoms are replaced by hydrogen atoms in a certain probability during purification. Of 3729 hydrogen atoms, 2932 are nonexchangeable C-H hydrogen atoms and 337 are N-H or O-H of the side chains which are likely to be exchangeable and 460 are N-H on the main-chain which would be partly exchangeable. Supposing 30% of the main-chain hydrogen atoms are nonexchangeable, 138 out of 460 main-chain deuterium atoms remain in the protein. Thus 3070 (2932 plus 138) hydrogen atoms would be nonexchangeable. The difference in masses between CueO-d and CueO-h is 3104, indicating that the deuteration ratio is almost 100%, if ignoring the effect of the back-replacement of deuterium after purification. Supposing all the exchangeable hydrogen atoms were back-replaced by deuterium in the deuterated buffer solution, deuteration ratio is calculated to be 83.2%.

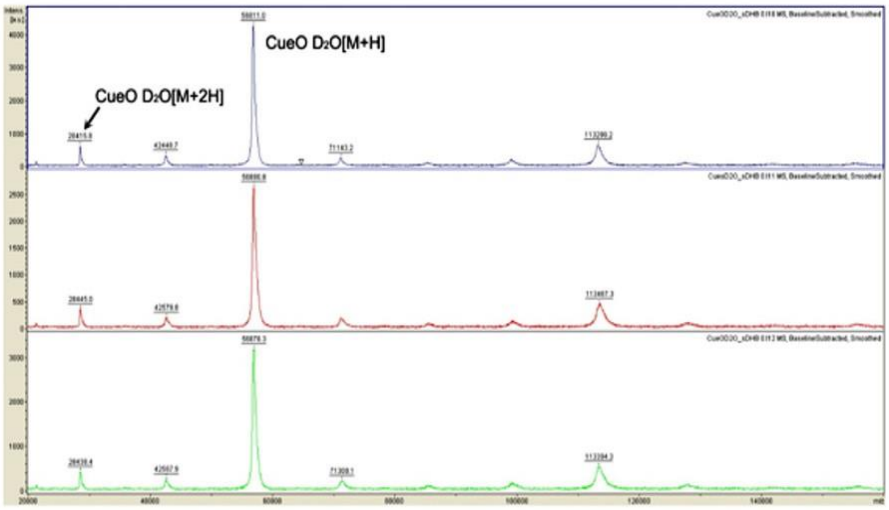

(A)

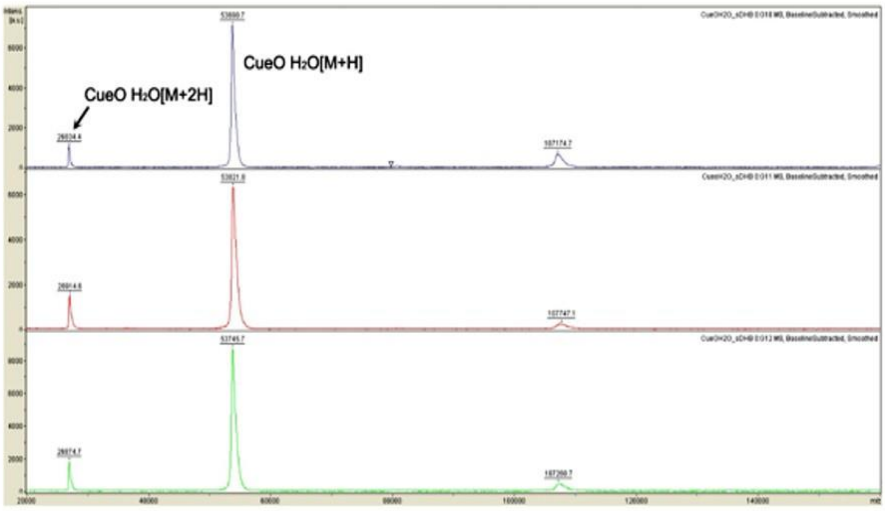

(B)

Fig. 20. MALDI-TOF mass spectra of A) CueO-d B) CueO-h.

Table 4. Summary of MALDI-TOF mass spectrometry results.

Measurement	Peak (*m*/*z*)			
	CueO-d		**CueO-h**	
	$[M+H]^+$	$[M+2H]^{2+}$	$[M+H]^+$	$[M+2H]^{2+}$
1	56811.0	28415.8	53690.7	26834.4
2	56880.8	28445.0	53821.8	26914.6
3	56878.3	28438.4	53745.7	26874.7
Average	56856.7	28433.1	53752.7	26874.6
Difference between CueO-d and CueO-h	3104.0	1558.5	–	–

3.12. Crystallization

3.12.1. Screening of the crystallization condition for oCueO-h and CueO-h

Crystals of oCueO-h and CueO-h were obtained from the solutions of the several screening precipitants, but the most of the crystals were in tiny size **(Fig. 21)**.

A.

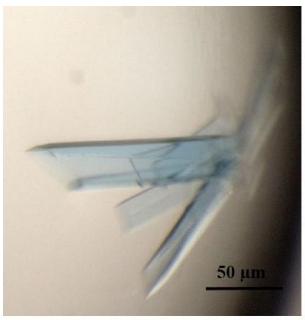

Protein conc^{n}: 6 mg/ mL
Temperature: 20^{o}C
Crystallization condition
0.2 M lithium chloride
0.1 M sodium acetate; pH 5.0
20 % (w/v) PEG 6000

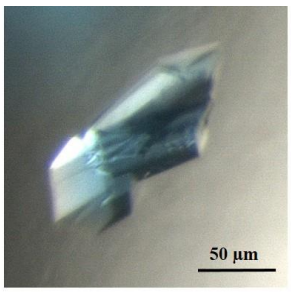

Protein conc^{n}: 6 mg/ mL
Temperature: 20^{o}C
Crystallization condition
0.2 M sodium chloride
0.1 M HEPES; pH 7.0
20 % (w/v) PEG 6000

B.

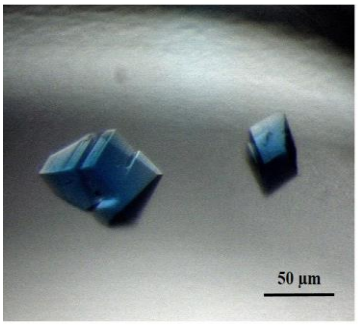

Protein conc^{n}: 6 mg/ mL
Temperature: 20^{o}C
Crystallization condition
0.2 M Calcium chloride dehydrate
0.1 M MES: pH 6.0
20 % (w/v) PEG 6000

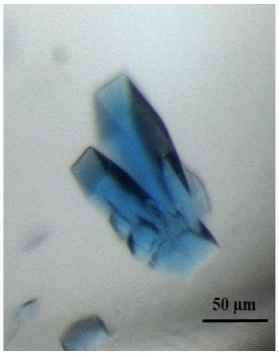

Protein conc^{n}: 6 mg/ mL
Temperature: 20^{o}C
Crystallization condition
0.2 M Imidazole malate; pH7.0
20% (w/v) PEG 4000

Fig. 21. Crystals of (A) oCueO-h and (B) CueO-h.

3.12.2. Crystals from the optimization of the precipitants

Larger and well-shaped single crystals of oCueO-h and CueO-h were obtained from the optimized conditions **(Fig. 22)**.

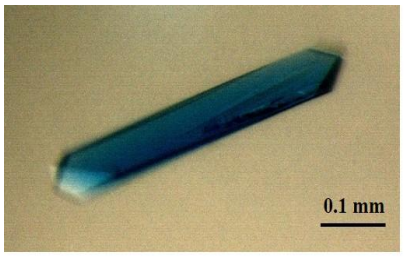

Protein conc^{n}: 6 mg/ mL

Temperature: 4^{o}C

Crystallization condition

0.2 M sodium chloride
0.1 M HEPES; pH 7.0
18 % (w/v) PEG 6000

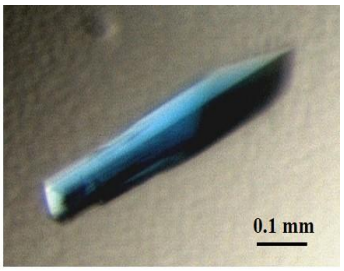

Protein conc^{n}: 6 mg/ mL

Temperature: 20^{o}C

Crystallization condition

0.2 M lithium chloride
0.1 M HEPES; pH 7.0
20 % (w/v) PEG 6000

A.

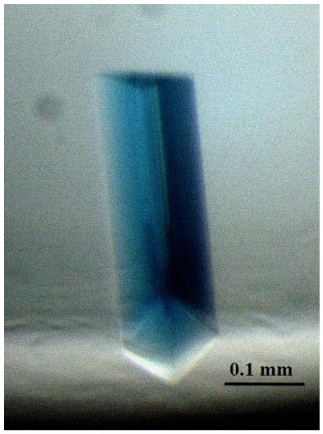

Protein conc^{n}: 6 mg/ mL

Temperature: 20^{o}C

Crystallization condition

0.2 M Ammonium sulfate
12 % (w/v) PEG 8000

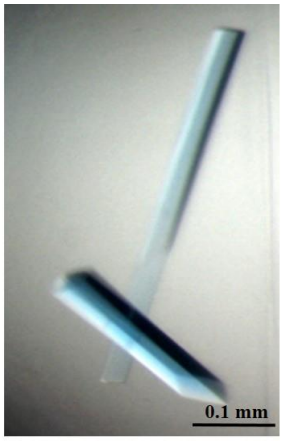

Protein conc^{n}: 6 mg/ mL

Temperature: 20^{o}C

Crystallization condition

0.2 M Ammonium sulfate
0.1 M Tris; pH 8.5
12 % (w/v) PEG 8000

B.

Fig. 22. Crystals of (A) oCueO-h and (B) CueO-h in optimized conditions.

3.12.3. Crystals of the oCueO-d and CueO-d

The crystals of deuterated CueO in selected conditions were better in size and shape. However, the CueO-d crystals were thicker than those of oCueO-d **(Fig. 23)**.

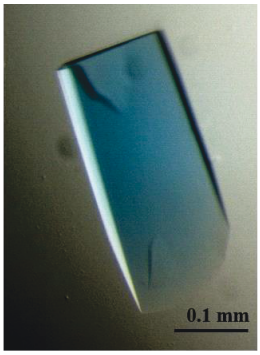

Protein conc^{n}: 6 mg/ mL
Temperature: 20^{o}C
Crystallization condition
0.1 M Na HEPES; pD 7.0
14 % (w/v) PEG 8000

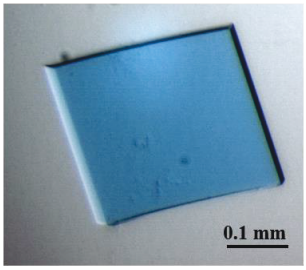

Protein conc^{n}: 6 mg/ mL
Temperature: 20^{o}C
Crystallization condition
0.1 M Na HEPES; pD 7.0
16 % (w/v) PEG 8000

A.

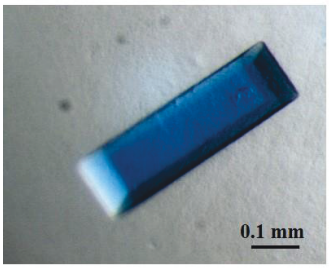

Protein conc^{n}: 6 mg/ mL
Temperature: 4^{o}C
Crystallization condition
0.2 M Calcium chloride dehydrate
0.1 M HEPES; pD 7.0
16 % (w/v) PEG 6000

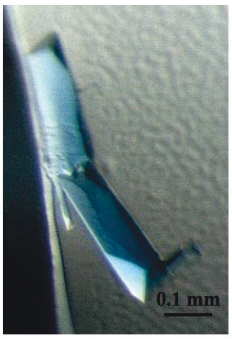

Protein conc^{n}: 6 mg/ mL
Temperature:20^{o}C
Crystallization condition
0.2 M lithium chloride
0.1 M HEPES; pD 7.0
20 % (w/v) PEG 6000

B.

Fig. 23. Crystals of (A) oCueO-d and (B) CueO-d.

3.13. X-ray diffraction experiment

The oCueO-d, CueO-h, and CueO-d crystals were diffracted to 1.42, 1.45, and 1.80 Å, respectively **(Fig. 24)**.

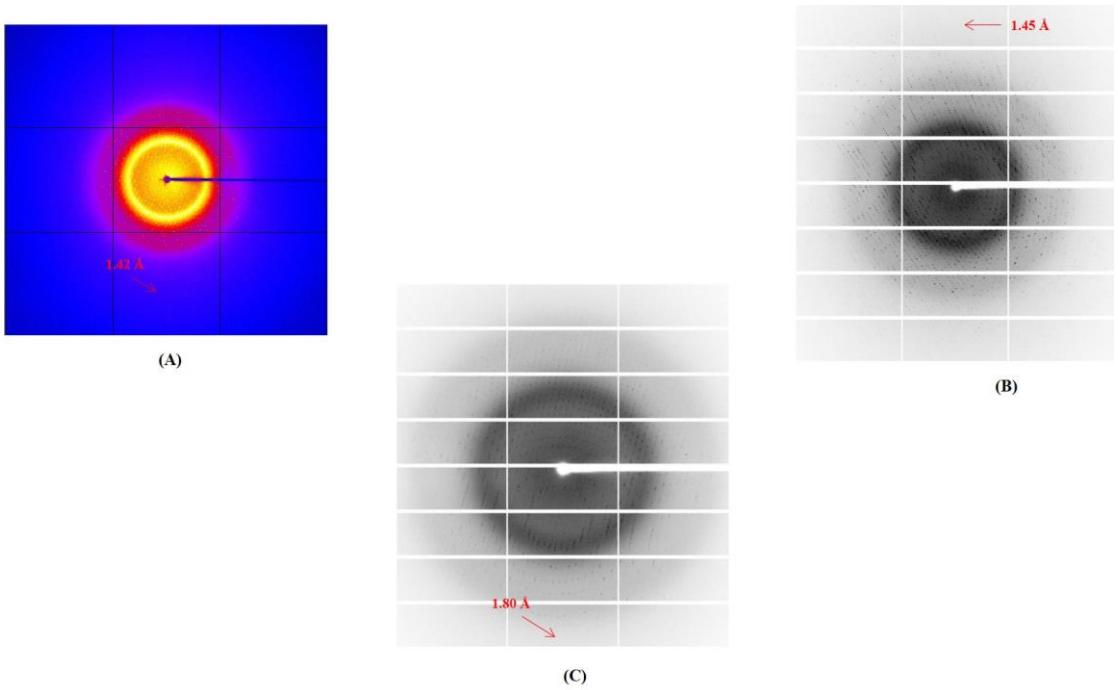

Fig. 24. X-ray diffraction patterns of (A) oCueO-d, (B) CueO-h, and (C) CueO-d, crystals.

3.14. X-ray structures of oCueO-d, CueO-h, and CueO-d

Crystals obtained from the precipitating agents of 0.1 M Na HEPES pD 7.0, 14% (w/v) PEG 8000 for oCueO-d, and in 0.2 M calcium chloride dihydrate, 0.1 M MES pH 6.0, and 20% (w/v) PEG 6000 for CueO-h, and in 0.2 M lithium chloride, 0.1 M HEPES pD 7.0, and 20% (w/v) PEG 6000 for CueO-d, were used to perform X-ray diffraction

experiment. The structures of oCueO-d, CueO-h, and CueO-d were solved at 1.42, 1.45, and 1.80 Å, respectively **(Fig. 25)**. By introducing the HRV3C cleavage site just after the signal sequence, I obtained high-resolution diffractive crystals for the non-deuterated and deuterated enzymes. For CueO-d, I obtained crystals that were thicker than those of oCueO-d. CueO-h crystallized in the $P2_1$ space group with cell dimensions of a = 49.51 Å, b = 88.79 Å, c = 53.95 Å, and β = 94.24° like other previously reported non-deuterated wild-type CueO crystals (Roberts *et al*., 2002; Roberts *et al*., 2003; Singh *et al*., 2011; Komori *et al*., 2012; Komori *et a*l., 2013 & Komori *et al*., 2014). However, CueO-d crystallized in the $P2_12_12_1$ space group with cell dimensions of a = 49.91 Å, b = 106.92 Å, and c = 262.89 Å as well as oCueO-d crystallized in the $P2_12_12_1$ space group with cell dimensions of a = 52.32 Å, b = 70.42 Å, and c = 134.0 Å. The data collection and refinement statistics of these three crystals are summarized in **Table 5.** The values of R_{work}, R_{free}, and other geometrical statistics showed that the structures were well refined.

Table 5. Data collection and refinement statistics.

Data collection	**oCueO-d**	**CueO-h**	**CueO-d**
Beamline	BL38B1, SPring-8	NE3A, Photon Factory	NE3A, Photon Factory
Wavelength (Å)	1.0000	1.0000	1.0000
Space group	$P2_1\ 2_1\ 2_1$	$P2_1$	$P2_1\ 2_1\ 2_1$
Cell axes (Å)	52.32, 70.42, 134.03	49.51, 88.79, 53.95	49.91, 106.92, 262.89
Cell angles (°)	90, 90, 90	90, 94.24, 90	90, 90, 90
Resolution (Å)	50.0-1.42	50.0 – 1.45	50.0 -1.80

R_{merge} (%)	5.80 (97.7)	10.8 (60.1)	12.1 (88.4)
Mean $I/\sigma I$	16.4 (1.95)	10.7 (2.84)	9.70 (2.55)
Completeness (%)	99.8 (98.3)	99.8 (96.8)	99.7 (98.3)
Redundancy	6.3 (6.2)	6.3 (5.0)	6.4 (5.4)
Number of total reflections	593343	522228	834703
Number of unique reflections	94351 (9168)	82325 (7928)	131193 (12758)
Wilson B-factor (Å^2)	15.5	12.7	21.5
Refinement			
Resolution (Å)	31.2-1.42 (1.47-1.42)	35.1-1.45 (1.50-1.45)	37.5-1.80 (1.86-1.80)
R_{work}	0.156 (0.237)	0.153 (0.222)	0.166(0.246)
R_{free}	0.183 (0.272)	0.181 (0.263)	0.204 (0.276)
Number of non-hydrogen atoms (protein)	4282	4154	11511
Mean B value (Å^2)	22.70	17.80	30.00
Number of waters	558	485	763
rmsd bond lengths (Å)	0.006	0.006	0.007
rmsd bond angles (°)	1.15	1.14	1.10
Ramachandran plot			
Residues in favoured regions (%)	97	97	97
Residues in allowed regions (%)	3	3	3
Residues in disallowed regions (%)	0	0	0

* $R_{merge} = \sum_{hkl}\sum_i |I_i\ (hkl) - \langle I(hkl)\rangle| \ / \ \sum_{hkl}\ \sum I_i(hkl)$, where $I_i(hkl)$ is the intensity of the ith observation. **Numbers in parentheses are for the highest-resolution shell

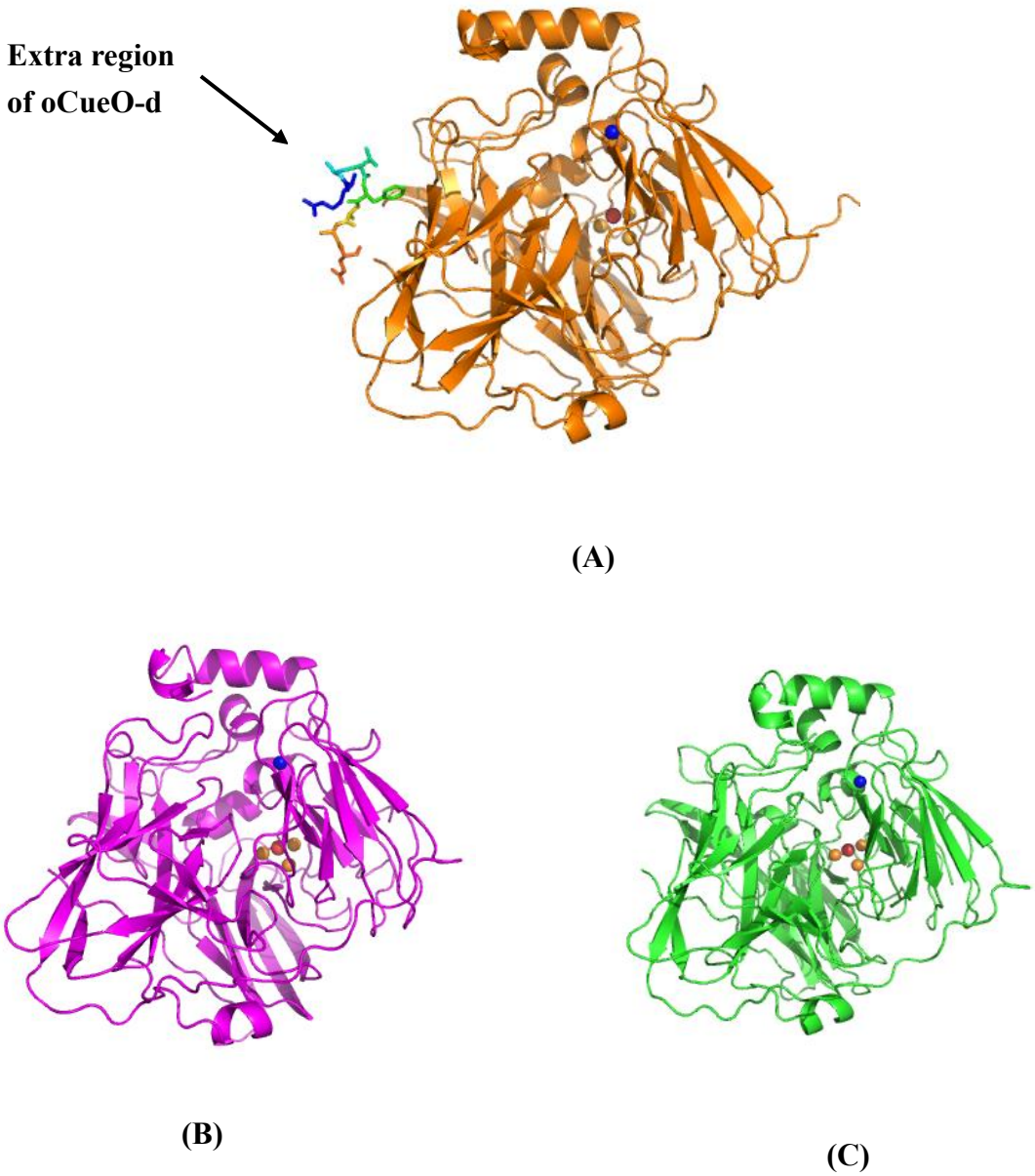

Fig. 25. X-ray structures of (A) oCueO-d, (B) CueO-h, and (C) CueO-d, with the T1 Cu and trinuclear Cu center (TNC) shown as space-filling spheres. The overall structure of these CueO proteins (oCueO-d, CueO-h, CueO-d) is almost similar except an extra 7-residue in N-terminal site in oCueO-d structure (shown in stick model).

3.15. Comparison of the X-ray structures of oCueO-d, CueO-d, and CueO-h

Structural comparison of the CueOs **(Fig. 26)** showed that there was no significant difference in the overall structure except for the N-terminal region of the oCueO-d, which was not observed in CueO (1KV7), CueO-d, and CueO-h. The N-terminus of oCueO-d contained extra residues (RAVFAAE-) derived from the signal sequence. These extra residues may have affected the crystal packing and prevented large single crystals suitable for neutron diffraction from forming. The residue is likely attributed to the inhibition of the cleavage of the signal sequence by deuteration of oCueO when it is transferred from the cytoplasmic to periplasmic space. The mature CueO-h was easily extracted from the cells by osmotic shock because it was mainly located in the periplasmic space. The yields of oCueO-d obtained by osmotic shock were low; thus, it was extracted by sonication, suggesting that the bacterial cells did not contain large amounts of mature oCueO-d in the periplasmic space. As a result, I obtained a small amount of mature (signal-truncated), partially truncated, and untruncated premature oCueO-d by sonication from the periplasmic and cytoplasmic spaces during enzyme preparation. The mechanism of the inhibition of the enzymatic signal sequence cleavage by deuteration was unclear.

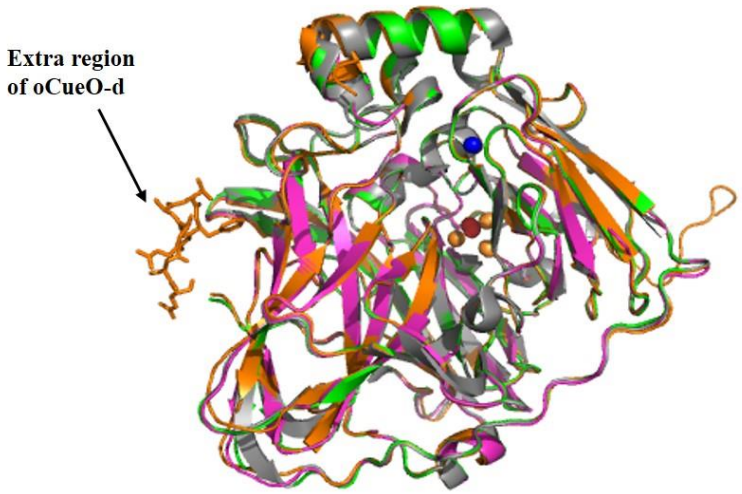

Fig. 26. Overall structure of CueO. T1 copper ions are shown as dark blue spheres, T2/T3 copper ions are shown as gold spheres, and water molecule of TNC are shown as red spheres. Previously published non-deuterated CueO (1KV7, gray)**,** oCueO-d (orange)**,** CueO-h (magenta), and CueO-d (green) are superimposed. The overall structures of CueO are almost identical, but the deuterated oCueO-d contains extra 7-residues in the N-terminal site (shown in stick).

3.16. Structure of the copper centers

CueO contains four copper ions, arranged in the T1 (one ion) site and T2 (one ion)/T3 (two ions) cluster. The T1 Cu is coordinated by His443, His505, Cys500, and Met510. The T2 Cu is coordinated by His101 and His446, whereas the two T3 Cu ions are coordinated by His103, His141, and His501; by His143, His448, and His499; and by a water molecule.

Superimposing CueO (1KV7), oCueO-d, CueO-h, and CueO-d demonstrates that despite the deuteration of the enzyme, the T1 **(Fig. 27 A)** and T2/T3 Cu clusters

(Fig. 27 B) are identical with average root-mean-square deviations of 0.08 and 0.12 Å, respectively. The distances between the copper ions and the ligand atoms **(Table 6)** indicate that deuteration of CueO does not alter the coordination geometry of the active site of the protein.

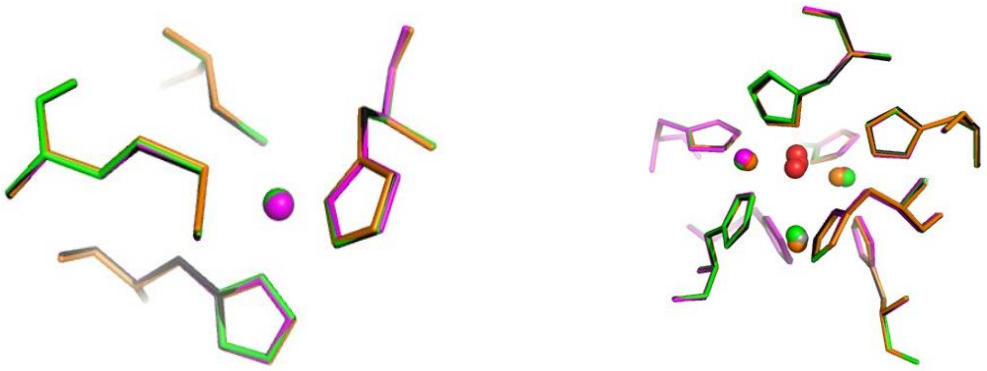

(A) **(B)**

Fig. 27. The copper centers of CueO.

T1 copper site **(A)** and T2/T3 copper site **(B)** CueO (1KV7, gray), oCueO-d (orange), CueO-h (magenta), and CueO-d (green) are superimposed.

Table 6. Copper-ligand distances (Å).

	CueO (PDB code 1KV7)	**oCueO-d**	**CueO-h**	**CueO-d**
T1 Cu – His 443	2.0	2.0	2.1	2.0
T1 Cu – Cys 500	2.2	2.2	2.2	2.2
T1 Cu – His 505	2.0	2.0	2.0	2.0
T1 Cu – Met 510	3.2	3.3	3.2	3.2
T2 Cu – His 101	1.9	2.0	1.7	1.9
T2 Cu – His 446	1.8	2.0	1.7	1.9
T3aCu – His 103	2.0	1.9	1.9	2.0
T3aCu – His 141	2.0	2.0	1.9	2.0
T3aCu – His 501	2.1	2.1	2.1	2.2
T3aCu – HOH	2.4	2.4	2.5	2.4
T3bCu – His 143	2.0	2.0	1.9	2.1
T3bCu – His 448	1.9	2.0	1.9	2.0
T3bCu – His 499	2.0	2.1	1.9	1.9
T3bCu – HOH	2.3	2.2	2.3	2.5
T2 Cu – T3aCu	4.0	4.1	4.0	3.9
T2 Cu – T3bCu	3.5	3.5	3.5	3.5
T3aCu – T3bCu	4.7	4.4	4.8	4.8

4. Conclusions

I established an expression system for deuterated CueO with an HRV3C cleavage site just after the signal sequence; the deuterated protein obtained from the original system had seven extra residues originating from the signal sequence. I developed an efficient purification procedure for CueO-d. Mass spectroscopy showed that the CueO samples were highly purified and deuterated, indicating that this is a candidate protein for obtaining sufficiently large, high-quality crystals for neutron diffraction studies. CueO-h and CueO-d from the new construct and o-CueO-d from the original construct were crystallized and their structures were solved by X-ray crystallography. The overall and active site structures, the spectroscopic and biochemical data showed that CueO-d and CueO-h had the same features as those of oCueO-h. Based on the biochemical and physiochemical data, the structure-function relationship of CueO is expected to be elucidated by neutron crystallography of the present CueO sample.

5. References

Adachi, M., Ohhara, T., Kurihara, K., Tamada, T., Honjo, E., Okazaki, N., Arai, S., Shoyama, Y., Kimura, K., Matsumura, H., Sugiyama, S., Adachi, H., Takano, K., Mori, Y., Hidaka, K., Kimura, T., Hayashi, Y., Kiso, Y. & Kuroki, R. Structure of HIV-1 protease in complex with potent inhibitor KNI-272 determined by high-resolution X-ray and neutron crystallography. *Proc. Natl. Acad. Sci. USA*, **2009**, *106*, 4641–4646.

Adams, P. D., Afonine, P. V., Bunkóczi, G., Chen, V. B., Davis, I. W., Echols, N., Headd, J.J., Hung, L.W., Kapral, G.J., Grosse-Kunstleve, R.W., McCoy, A.J., Moriarty, N.W., Oeffner, R., Read, R.J., Richardson, D.C., Richardson, J.S., Terwilliger, T.C. & Zwart P.H. PHENIX: a comprehensive Python-based system for macromolecular structure solution. *Acta Cryst. D*, **2010**, *66*, 213–221.

Adman, E. T. Copper protein structures. *Adv Protein Chem*., **1991**, *42*, 145–97.

Bento, I., Martins, L. O., Lopes, G. G., Carrondo, M. A. & Lindley, P. F. Dioxygen reduction by multi-copper oxidases; a structural perspective. *Dalton Trans*., **2005**, *21*, 3507–3513.

Blakeley, M. P., Ruiz, F., Cachau, R., Hazemann, I., Meilleur, F., Mitschler, A., Ginell, S., Afonine, P., Ventura, O. N., Cousido-Siah, A., Haertlein, M., Joachimiak, A., Myles, D. & Podjarny, A. Quantum model of catalysis based on a mobile proton revealed by subatomic X-ray and neutron diffraction studies of h-aldose reductase. *Proc. Natl. Acad. Sci. USA*, **2008**, *105*, 1844–1848.

Blakeley, M. P., Langan, P., Niimura, N. & Podjarny, A. Neutron crystallography: opportunities, challenges, and limitations. *Curr. Opin. Struct. Biol.*, **2008**, *18*, 593–600.

Bon, C., Lehmann, M. S. & Wilkinson, C. Quasi-Laue neutron-diffraction study of the water arrangement in crystals of triclinic hen egg-white lysozyme. *Acta Cryst. D*, **1999**, *55*, 978–987.

Budayova-Spano, M., Dauvergne, F., Audiffren, M., Bactivelane, T. & Cusacka, S. A methodology and an instrument for the temperature-controlled optimization of crystal growth. *Acta Cryst. D*, **2007**, *63*, 339–347.

Coates, L., Erskine, P. T., Wood, S. P., Myles, D. A. A. & Cooper, J. B. A neutron Laue diffraction study of endothiapepsin: implications for the aspartic proteinase mechanism. *Biochemistry*, **2001**, *40*, 13149–13157.

Coates, L., Tuan, H.-F., Tomanicek, S., Kovalevsky, A., Mustyakimov, M., Erskine, P. & Cooper, J. The catalytic mechanism of an aspartic proteinase explored with neutron and X-ray diffraction. *J. Am. Chem. Soc*., **2008**, *130*, 7235–7237.

DeLano, W. L. *The PyMOL Molecular Graphics Systems*, DeLano Scientific, San Carlos, CA, USA. **2002**. http://www.pymol.org.

Djoko, K. Y., Chong, L. X., Wedd, A. G. & Xiao, Z. Reaction Mechanisms of the

Multicopper Oxidase CueO from *Escherichia coli* Support Its Functional Role as a Cuprous Oxidase. *J. Am. Chem. Soc*., **2010**, *132*, 2005–2015.

Emsley, P. & Cowtan, K. Coot: model-building tools for molecular graphics. *Acta Cryst. D*, **2004**, *60*, 2126–2132.

Fisher, S. Z., Aggarwal, M., Kovalevsky, A. Y., Silverman, D. N. & McKenna, R. Neutron diffraction of acetazolamide-bound human carbonic anhydrase II reveals atomic details of drug binding. *J. Am. Chem. Soc*., **2012**, *134*, 14726–14729.

Flora, M., Parthapratim, M., Lee, R., Alexandru, D. S., Lowell, C., Andrey, K., Tibor, K., Bryan, C. C, Robert, B. & Dean, A. A. M. The IMAGINE instrument: first neutron protein structure and new capabilities for neutron macromolecular crystallography. *Acta Cryst. D*, **2013**, *69*, 2157–2160.

Gamble, T. R., Clauser, K. R. & Kossiakoff, A. A. The production and X-ray structure determination of perdeuterated Staphylococcal nuclease. *Biophys. Chem*., **1994**, *53*, 15–25.

Grass, G. & Rensing, C., CueO is a multi-copper oxidase that confers copper tolerance in *Escherichia coli*. *Biochem. Biophys. Res. Commun*., **2001**, *286*, 902-908.

Grass, G. & Rensing, C. Genes involved in copper homeostasis in *Escherichia coli*. *J. Bacteriol*., **2001**, *183*, 2145–2147.

Glusker, J. P., Carrell, H. L., Kovalevsky, A. Y., Hanson, L., Fisher, S. Z., Mustyakimov, M., Mason, S., Forsyth, T. & Langan, P. Using neutron protein crystallography to understand enzyme mechanisms. *Acta Cryst. D*, **2010**, *66*, 1257–1261.

Hazemann, I., Dauvergne, M. T., Blakeley, M. P., Meilleur, F., Haertlein, M., Van Dorsselaer, A., Mitschler, A., Myles, D. A. & Podjarny, A. High-resolution neutron protein crystallography with radically small crystal volumes: application of perdeuteration to human aldose reductase. *Acta Cryst. D*, **2005**, *61*, 1413–1417.

Kataoka, K., Komori, H., Ueki, Y., Konno, Y., Kamitaka, Y., Kurose, S., Tsujimura, S., Higuchi, Y., Kano, K., Seo, D. & Sakurai, T. Structure and function of the engineered multicopper oxidase CueO from *Escherichia coli*-deletion of the methionine-rich helical region covering the substrate-binding site. *J. Mol. Biol.*, **2007**, *373*, 141-52.

Kataoka, K., Sugiyama, R., Hirota, S., Inoue, M., Urata, K., Minagawa, Y., Seo, D. & Sakurai, T. Four-electron reduction of dioxygen by a multicopper oxidase, CueO, and roles of Asp^{112} and Glu^{506} located adjacent to the trinuclear copper center. *J. Biol. Chem*., **2009**, *284*, 14405–14413.

Kim, C., Lorenz, W. W., Hoopes, J. T. & Dean, J. F. Oxidation of phenolate siderophores by the multicopper oxidase encoded by the *Escherichia coli* yacK gene. *J. Bacteriol*., **2001**, *183*, 4866–4875.

Komori, H. & Higuchi, Y. Structure and molecular evolution of multicopper blue proteins. *BioMol Concepts*., **2010**, *1*, 31–40.

Komori, H., Sugiyama, R., Kataoka, K., Higuchi, Y. & Sakurai, T. An O-centered structure of the trinuclear copper center in the Cys500Ser/Glu506Gln mutant of CueO and structural changes in low to high X-ray dose conditions. *Angew. Chem. Int. Ed.*, **2012**, *51*, 1861-1864.

Komori, H., Kajikawa, T., Kataoka, K., Higuchi, Y. & Sakurai, T. Crystal structure of the CueO mutants at Glu506, the key amino acid located in the proton transfer pathway for dioxygen reduction. *Biochem. Biophysi. Res. Commun*., **2013**, *438*, 686–690.

Komori, H., Sugiyama, R., Kataoka, K., Miyazaki, K., Higuchi, Y. & Sakurai, T. New insights into the catalytic active-site structure of multicopper oxidases. *Acta Cryst. D*, **2014**, *70*, 772-779.

Kossiakoff, A. A. & Spencer, S. A. Neutron diffraction identifies His 57 as the catalytic base in trypsin. *Nature*, **1980**, *288*, 414-416.

Kossiakoff, A. A. & Spencer, S. A. Direct determination of the protonation states of aspartic acid-102 and histidine-57 in the tetrahedral intermediate of the serine proteases: neutron structure of trypsin. *Biochemistry*, **1981**, *20*, 6462-6474.

Kovalevsky, A., Hanson, B. L., Mason, S. A., Forsyth, V. T., Fisher, Z., Mustyakimov,

M., Blakeley, M. P., Keen, D. A. & Langan, P. Inhibition of D-xylose isomerase by polyols: atomic details by joint X-ray/neutron crystallography. *Acta Cryst. D*, **2012**, *68,* 1201–1206.

Li, X., Wei, Z., Zhang, M., Peng, X., Yu, G., Teng, M. & Gong, W. Crystal structures of *E. coli* laccase CueO at different copper concentrations. *Biochem. Biophys. Res. Commun.,* **2007**, *354*, 21-6.

Miura, Y., Tsujimura, S., Kamitaka, Y., Kurose, S., Kataoka, K., Sakurai, T. & Kano, K. Bioelectrocatalytic Reduction of O_2 catalyzed by CueO from *Escherichia coli* adsorbed on a highly oriented pyrolytic graphite electrode.*Chem. Lett.*, **2007**, *36*, 132–133.

Miura, Y., Tsujimura, S., Kurose, S., Kataoka, K., Sakurai, T. & Kano, K. Direct electrochemistry of CueO and its mutants at residues to and near type I Cu for oxygen-reducing biocathode. *Fuel Cells*, **2009**, *9*, 70–78.

Myles, D. A. A., Bon, C., Langan, P., Cipriani, F., Castagna, J. C. & Wilkinson, C. Neutron Laue diffraction in macromolecular crystallography. *Physica B*, **1998**, *241–243,* 1122–1130.

Niimura, N. & Bau, R. Neutron protein crystallography: beyond the folding structure of biological macromolecules. *Acta Cryst. A.*, **2008**, *64*, 12–22.

Otwinowski, Z. & Minor, W. Processing of X-ray diffraction data collected in

oscillation mode. *Methods Enzymol*, **1997**, *276*, 307-326.

Outten, F. W., Huffman, D. L., Hale, J. A. & O'Halloran, T. V. The independent *cue* and *cus* systems confer copper tolerance during aerobic and anaerobic growth in *Escherichia coli*. *J. Biol. Chem.*, **2001**, *276,* 30670-7.

Phillips, S. E. & Schoenborn, B. P. Neutron diffraction reveals oxygen-histidine hydrogen bond in oxymyoglobin. *Nature*, **1981,** *292,* 81-82.

Rensing, C. & Grass, G. *Escherichia coli* mechanisms of copper homeostasis in a changing environment. *FEMS Microbiol. Rev.*, **2003,** *27*, 197-213.

Roberts, S. A., Weichsel, A., Grass, G., Thakali, K., Hazzard, J. T., Tollin, G., Rensing, C. & Montfort, W. R. Crystal structure and electron transfer kinetics of CueO, a multicopper oxidase required for copper homeostasis in *Escherichia coli*., *Proc. Natl. Acad. Sci. USA*, **2002**, *99*, 2766-2771.

Roberts, S. A., Wildner, G. F., Grass, G., Weichsel, A., Ambrus, A., Rensing, C. & Montfort, W. R. A labile regulatory copper ion lies near the T1 copper site in the multicopper oxidase CueO. *J. Biol. Chem*., **2003**, *278*, 31958-63.

Sakurai, T. & Kataoka, K. Structure and function of type I copper in multicopper oxidases. *Cell. Mol. Life Sci.*, **2007**, *64*, 2642–2656.

Schoenborn, B. P. Neutron diffraction analysis of myoglobin. *Nature*, **1969**, *224*, 143-146.

Shu, F., Ramakrishnan, V. & Schoenborn, B. P. Enhanced visibility of hydrogen atoms by neutron crystallography on fully deuterated myoglobin. *Proc. Natl. Acad. Sci. USA*, **2000**, *97*, 3872–3877.

Singh, S. K., Roberts, S. A., McDevitt, S. F., Weichsel, A., Wildner, G. F., Grass, G. B., Rensing, C. & Montfort, W.R. Crystal structures of multicopper oxidase CueO bound to copper(I) and silver(I): functional role of a methionine-rich sequence. *J. Biol. Chem.*, **2011**, *286*, 37849–37857.

Solomon, E. I., Sundaram, U. M. & Machonkin, T. E. Multicopper oxidases and oxygenases. *Chem. Rev.*, **1996**, *96*, 2563-2606.

Solomon, E. I., Augustine, A. J. & Yoon, J. O_2 reduction to H_2O by the multicopper oxidases. *Dalton Trans.*, **2008**, *30*, 3921–3932.

Tomanicek, S. J., Wang, K. K., Weiss, K. L., Blakeley, M. P., Cooper, J., Chen, Y. & Coates, L. The active site protonation states of perdeuterated Toho-1 β-lactamase determined by neutron diffraction support a role for Glu166 as the general base in acylation. *FEBS Lett.,* **2011**, *585*, 364–368.

Tsujimura, S., Miura, Y. & Kano, K. CueO-immobilized porous carbon electrode exhibiting improved performance of electrochemical reduction of dioxygen to water. *Electrochimi. Acta*, **2008**, *53*, 5716–5720.

Ueki, Y., Inoue, M., Kurose, S., Kataoka, K. & Sakurai, T. Mutations at Asp112 adjacent to the trinuclear Cu center in CueO as the proton donor in the four-electron reduction of dioxygen. *FEBS Lett*., **2006**, 580, 4069–4072.

6. Acknowledgements

Giving all glory to God for His many blessings, whom without I could not have completed this long journey. The work took longer than what I expected, but I'm glad it's finally behind me and now I can continue to another chapter in my life.

I offer my sincerest gratitude and respect to my supervisor, Professor Dr. Yoshiki Higuchi for giving me the opportunity to work in his laboratory as a graduate student. He patiently provided the vision, encouragement and advice necessary for me to proceed through the doctoral program and complete my dissertation. His attention, knowledge and moral support always useful for my study. He is a role model for me.

I am also grateful to my mentor Professor Dr. Naoki Shibata for his valuable instruction, guidance and supervision throughout my experiments in this study. This thesis would not have been possible without his help and support.

A big thank goes to Professor Dr. Hirufomi Komori who taught me most of the experiments when I was a beginner. My special thanks belong to all the members of our laboratory for making an immense place to work and for a great help during my experiments and especially for a great time spending together.

I also would like to thank our collaborators Professor. Dr. Takeshi Sakurai and Dr. Kunishige Kataoka from Kanazawa University. I extend my thanks to Dr. Kiyohito Kihira from JAXA for his help with the mass spectrometric analyses and the beamline staff of SPring-8 for their help during data collection.

Finally, I would like to acknowledge the support of my family and friends. My family has been my rock of encouragement and love. I am very grateful to my family and especially to my husband Mahabub Zaman for his patience, great help and every day support.